Regional hydrocarbon potential and thermal reconstruction of the Lower Jurassic to lowermost Cretaceous source rocks in the Danish Central Graben

NIELS HEMMINGSEN SCHOVSBO, LOUISE PONSAING, ANDERS MATHIESEN, JØRGEN A. BOJESEN-KOEFOED, LARS KRISTENSEN, KAREN DYBKJÆR, PETER JOHANNESSEN, FINN JAKOBSEN & PETER BRITZE

Geological Society of Denmark
https://2dgf.dk

Received 15 April 2020
Accepted in revised form
7 August 2020
Published online
14 September 2020

Schovsbo, N.H., Ponsaing, L., Mathiesen, A., Bojesen-Koefoed, J.A., Kristensen, L., Dybkjær, K., Johannessen, P., Jakobsen, F. & Britze, P. 2020. Regional hydrocarbon potential and thermal reconstruction of the Lower Jurassic to lowermost Cretaceous source rocks in the Danish Central Graben. Bulletin of the Geological Society of Denmark, Vol. 68, pp. 195–230. ISSN 2245-7070.
https://doi.org/10.37570/bgsd-2020-68-09

The Danish part of the Central Graben (DCG) is one of the petroliferous basins in the offshore region of north-western Europe. The source rock quality and maturity is here reviewed, based on 5556 Rock-Eval analyses and total organic carbon (TOC) measurements from 78 wells and 1175 vitrinite reflectance (VR) measurement from 55 wells, which makes this study the most comprehensive to date. The thermal maturity is evaluated through 1-D basin modelling of 46 wells. Statistical parameters describing the distribution of TOC, hydrocarbon index (HI) and T_{max} are presented for the Lower Jurassic marine Fjerritslev Formation, the Middle Jurassic terrestrial-paralic Bryne, Lulu, and Middle Graben Formations and the Upper Jurassic to lowermost Cretaceous marine Lola and Farsund Formations in six areas in the DCG. For the Farsund Formation the source-rock richness is presented for selected stratigraphic sequences. The upper part of the Farsund Formation is immature in the southern part of the Salt Dome Province, and late oil mature in and near the Tail End Graben and in the Søgne Basin. The lower part of the Farsund Formation is immature in local areas, yet post-mature in the Tail End Graben and in the Salt Dome Province. The Lower and Middle Jurassic shales are gas-prone in most of the DCG. The depth of the oil window, as defined by a VR of 0.6% R_o, ranges between 2200 and 4500 m. The variations are ascribed to heat flow differences in the DCG and can be modelled by a simple depth model, which includes the thickness of the Cretaceous to Palaeogene Chalk and Cromer Knoll Groups. According to the model, a thick Chalk Group offsets the oil window to deeper levels, which likely can be attributed to the thermal properties of the highly thermally conductive chalk compared to the underlying less thermally conductive clays. The DCG is an overpressured basin, and high-pressure, high-temperature conditions are expected to occur deeper than 3.8 km except for the Feda and Gertrud Grabens where such conditions, due to generally lower temperatures, are expected to occur deeper than around 4.7 km.

Keywords: Danish Central Graben, Basin modelling, Jurassic source rock quality and maturation, vitrinite reflectance modelling.

Niels Hemmingsen Schovsbo [nsc@geus.dk], Louise Ponsaing [louise.ponsaing@gmail.com], Anders Mathiesen [anm@geus.dk], Jørgen A. Bojesen-Koefoed [jbk@geus.dk], Lars Kristensen [lk@geus.dk], Karen Dybkjær [kd@geus.dk], Peter Johannessen [pjo@geus.dk], Finn Jakobsen [fj@geus.dk], Peter Britze [pbr@geus.dk], all Geological Survey of Denmark and Greenland (GEUS), Øster Voldgade 10, DK-1350 Copenhagen K, Denmark.

The Danish Central Graben (DCG) is part of the North Sea rift basin (Fig. 1). The main petroleum source rocks of this mature petroleum province are the Upper Jurassic – lowermost Cretaceous marine shales, which are referred to as the Farsund Formation in the DCG, the Kimmeridge Clay Formation in the UK sector and the Mandal Formation in the Norwegian part of the Central Graben (Damtoft *et al.* 1987, 1992; Ineson *et al.* 2003; Petersen *et al.* 2010, 2012; Verreussel *et al.* 2018). The Middle Jurassic coaly units of the Bryne and Lulu

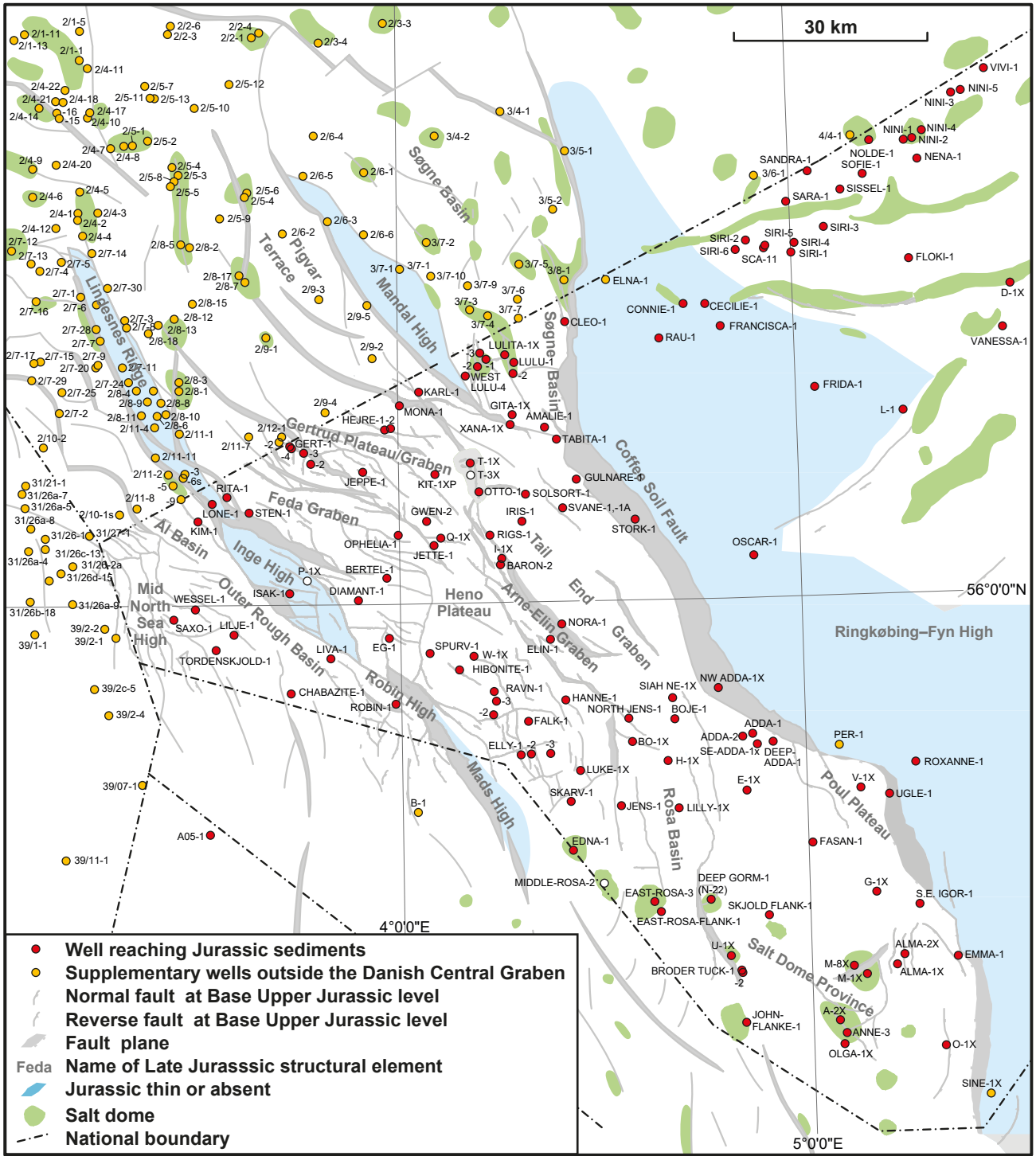

Fig. 1. Structural elements and wells that reach the Jurassic sediments in the southern part of the Central Graben. Updated from Japsen *et al.* (2003). For wells included in this study, see Table 1.

Formations constitute a secondary source, whereas unknown contribution may come from other source rocks including the Upper Jurassic Lola Formation, the Lower Jurassic Fjerritslev Formation, Permian shales and Carboniferous coals (Damtoft *et al.* 1987, 1992; Petersen & Nytoft 2007a,b; Petersen *et al.* 2016; Petersen & Hertle 2018).

The Jurassic – lowermost Cretaceous source rocks mainly charged the Cretaceous – Palaeogene Chalk Group from where the main hydrocarbon production occurs in the DCG (Fig. 2). Secondary production occurs from Middle Jurassic and Palaeogene sandstones and more recently also from Upper Jurassic and Miocene sandstones (Goffey *et al.* 2018; Pedersen *et al.* 2018). Exploration of other Upper Jurassic plays has led to the Hejre-1, Amalie-1, Svane-1 and Xana-1X high-pressure and high-temperature (HPHT) discoveries (Fig. 2). These discoveries were made in fan delta sandstones and offshore gravity flow deposits (Fig. 3). More recently, a growing interest has been seen for unconventional hydrocarbon resources within the Jurassic shales in the DCG (Galluccio *et al.* 2019). Efforts to map and quantify the resources in Central Graben have begun as part of the project Geological Analysis and Resource Assessment of selected Hydrocarbon systems (GARAH: Schovsbo *et al.* 2020).

The first regional review of the quality and maturity of all Jurassic source rocks in the DCG was presented by Damtoft *et al.* (1987). Since then, the amount of source rock data and the regional stratigraphic knowledge has advanced considerably, with Ineson & Surlyk (2003) being a major milestone. A second major advancement in our understanding was gained from the 'Jurassic Petroleum System Project' (PETSYS) completed in 2014, which allowed integration of the seismic, bio- and lithostratigraphic framework for the Jurassic. In this project, geochemical databases on source rock quality, maturity and oil geochemistry were key results, allowing detailed integrated studies to be made. Important results from this project have been published by Johannessen *et al.* (2010) on sedimentology and by Petersen *et al.* (2010, 2011, 2012, 2013) and more recently Ponsaing *et al.* (2018, 2020a,b) on source rock quality and maturity.

The remaining challenge in the DCG is to provide a regional overview of the source rock quality and maturity. The present paper aims to refine the geochemical characterization of the Jurassic source rock succession by integrating source rock geochemistry with a sequence stratigraphic framework; to map the maturity of the Jurassic source rocks based on 1-D basin maturity models; and to examine the relationship between the chalk thickness and the position of the oil window as outlined by Petersen *et al.* (2012).

Geological setting

The North Sea rift complex is a major east-dipping half-graben system consisting of a series of minor NW–SE trending half-grabens, which are bounded by the Coffee Soil Fault to the east and the Mid North Sea High to the west (Fig. 1; Andsbjerg & Dybkjær 2003; Møller & Rasmussen 2003; Japsen *et al.* 2003; Petersen *et al.* 2011, 2012).

The lithostratigraphy for the Jurassic to Neogene in the DCG is presented in Fig. 2. The Jurassic succession has been subdivided into 18 sequences based on integration of seismic stratigraphy and bio- and lithostratigraphy (Andsbjerg & Dybkjær 2003; Johannessen *et al.* 2010). In the Early Jurassic the DCG was characterized by a relatively slow sea level rise and deposition of the grey, shallow-marine shales of the Fjerritslev Formation (Figs 3 and 4A; Michelsen *et al.* 2003). During the latest Early Jurassic – earliest Middle Jurassic the area was uplifted and the Triassic and most of the Lower Jurassic succession was removed by erosion (e.g. Andsbjerg & Dybkjær 2003; Møller & Rasmussen 2003). Due to this Toarcian erosion, parts of the Fjerritslev Formation are not present in the DCG (Fig. 3).

Mid-Jurassic rifting caused fault-controlled subsidence in the east, particularly along N–S trending segments of the Coffee Soil Fault (e.g. Japsen *et al.* 2003; Møller & Rasmussen 2003; Johannessen *et al.* 2010; Petersen *et al.* 2011). Because of the renewed subsidence and subsequent flooding of the DCG, the lower part of the Middle Jurassic is dominated by fluvial-channel sandstones assigned to the Bryne Formation (Fig. 4B). The upper part is characterized by paralic sandstones, shales and coal beds, which are overlain by shoreface and back-barrier deposits. These sediments are, however, restricted to the Søgne Basin, the Tail End Graben and the Salt Dome Province (Fig. 1). The paralic and marginally marine upper part is generally referred to the Lulu Formation in the north and to the Middle Graben Formation in the south. The base of the Middle Jurassic strata overlies the Mid-Cimmerian Unconformity or the Intra-Aalenian Unconformity (Michelsen *et al.* 2003; Petersen *et al.* 2011; Petersen & Hertle 2018).

During Oxfordian – Kimmeridgian, deep-water conditions were created in the DCG and the marine shales of the Lola Formation were deposited (Fig. 4C). The tectonic trend shifted in the Kimmeridgian from dominantly N–S to NW–SE oriented faulting and at the same time subsidence rates increased. The shallow-marine and back-barrier sandstones of the Heno Formation were deposited on the Heno and Gertrud plateaus during the late Kimmeridgian. The depositional area gradually extended westwards and

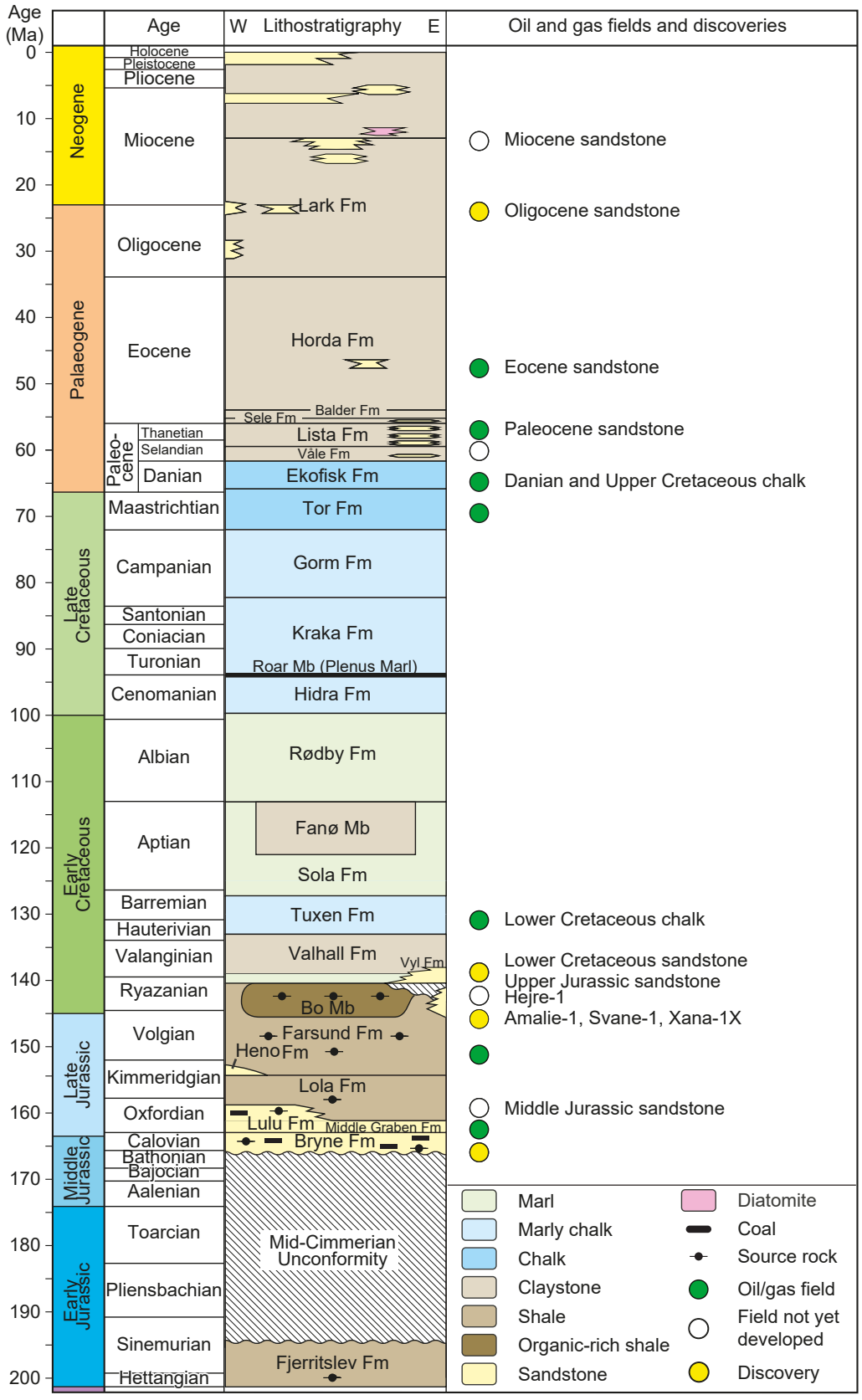

Fig. 2. Chronostratigraphy and lithostratigraphy of the Jurassic – Neogene in the Danish Central Graben with stratigraphic age and type of oil and gas fields and discovery wells mention in the text. Stratigraphy after Andsbjerg & Dybkjær (2003), Michelsen *et al.* (2003), Hemmet (2005) and van Buchem *et al.* (2018). Modified from Ponsaing *et al.* (2020b).

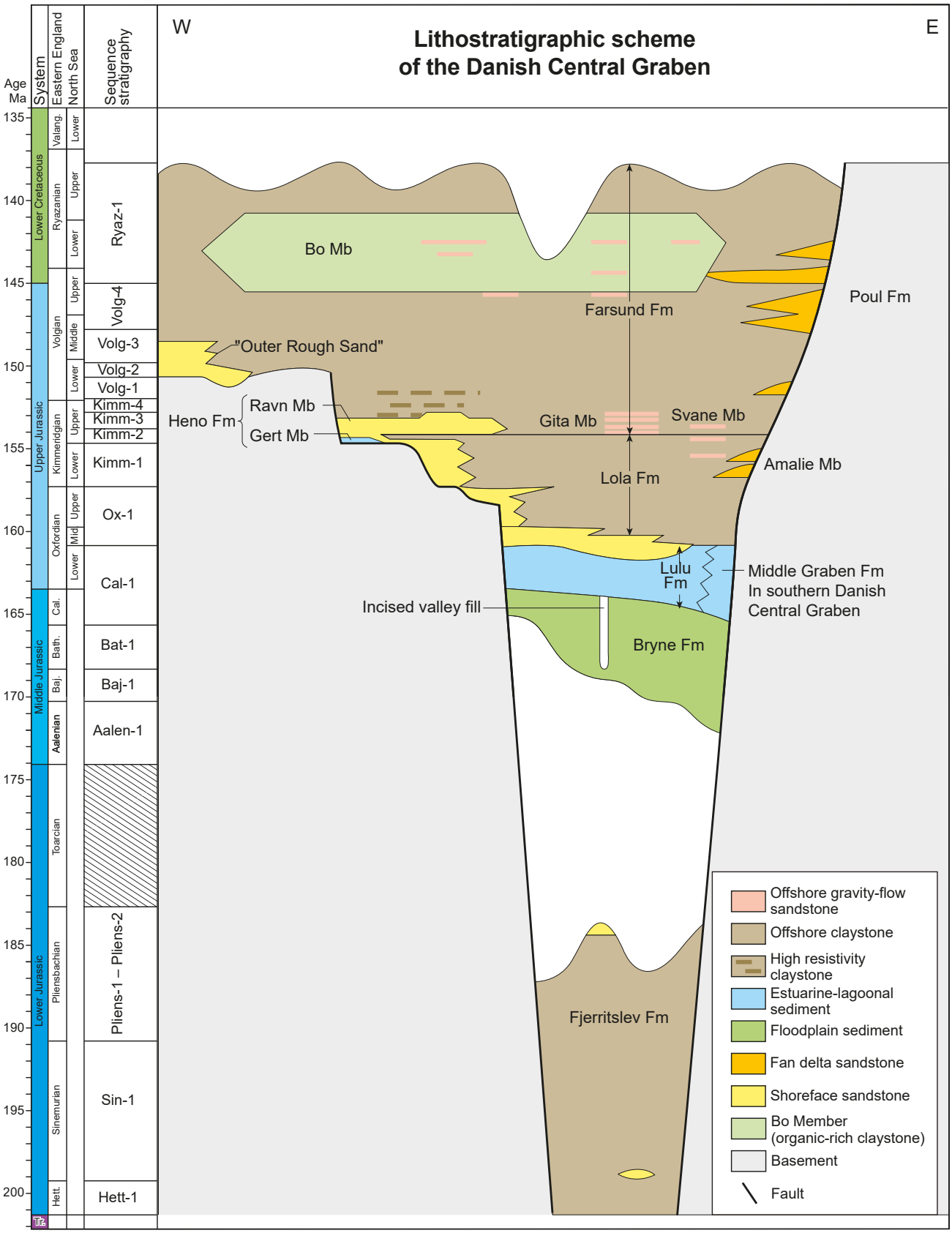

Fig. 3. Lithostratigraphic scheme of a west – east section trough the Danish Central Graben.

the thick, shale-dominated marine succession of the Farsund Formation was deposited over larger areas (Fig. 4D). During early Volgian, the overall transgression reached the Outer Rough and Ål basins (e.g. Andsbjerg & Dybkjær 2003; Johannessen *et al.* 2010; Petersen *et al.* 2011, 2012).

The subsidence rates were radically reduced in the latest Volgian, and the deposition of the organic-rich and highly radioactive 'hot shales' of the Bo Member (Volgian – Ryazanian) took place in most areas of the DCG (Fig. 3; Ineson *et al.* 2003; Michelsen *et al.* 2003).

The transition from the Farsund Formation to the overlying Cromer Knoll Group (Valhall to Rødby Formation, Fig. 2) marks a basinwide facies change from organic-rich shales to carbonate-rich and organic-lean shales deposited in open-marine environments. This transition is generally termed the Base Cretaceous Unconformity (BCU). The boundary marks the base of the deposits of the post-rift phase in the DCG, represented by the Cromer Knoll and Chalk Groups. In the Late Cretaceous to early Palaeogene, high sea level prevailed and the sedimentation shifted from siliciclastics to chalk composed of calcareous nanofossils (Anderskouv & Surlyk 2011; van Buchem *et al.* 2017) and to a compressional tectonic regime.

The thickness of the Chalk Group (Hidra to Ekofisk Formations, Fig. 2) varies from less than 200 m on inverted ridges to more than 1000 m in local depocentres

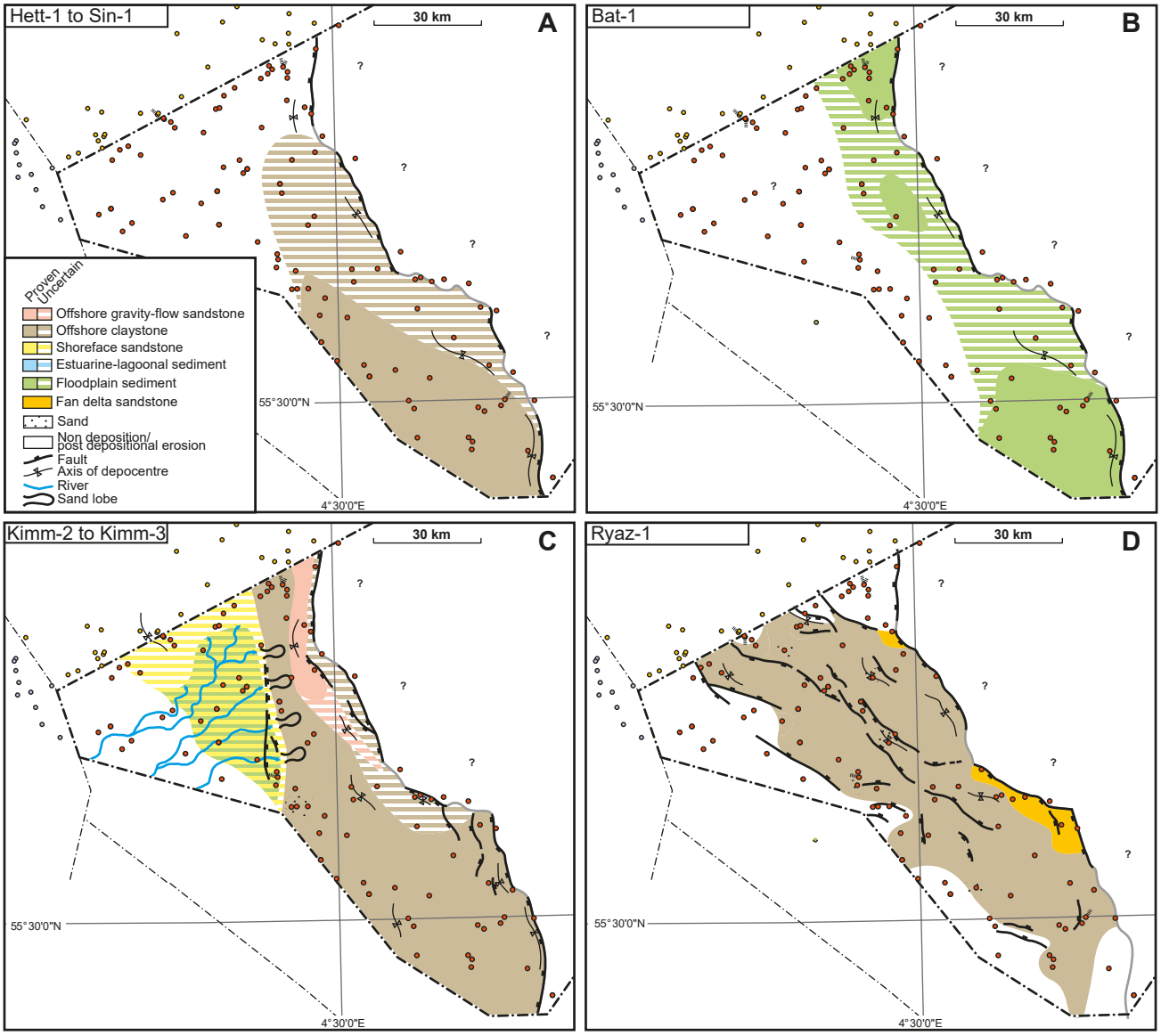

Fig. 4. Selected palaeogeography maps. **A:** The Lower Jurassic Hett-1 to Sin-1 sequences. **B:** The Middle Jurassic Bat-1 sequence. **C:** The Upper Jurassic Kimm-2 to Kimm-3 sequences. **D:** The Lower Cretaceous Ryaz-1 sequence. Modified from Andsbjerg & Dybkjær (2003) and Ponsaing *et al.* (2018).

in northern Tail End Graben, the Gertrud Graben and on the Heno Plateau (Fig. 5D). Deep burial of the Jurassic succession took place in the Paleocene to Neogene (Rasmussen *et al*. 2005), and the depth to the top of the Chalk Group and top Jurassic ranges from 1600 to 3400 m and 2200 to 5000 m, respectively (Fig. 5).

Database, analytical methods and modelling

Source rock, pressure and temperature databases

The source rock and vitrinite reflectance (VR) data used here consist mostly of data produced by the Geological Survey of Denmark and Greenland (GEUS) during the last almost four decades, but also include quality-controlled data reported from other sources. The Total Organic Carbon (TOC) and Rock-Eval data consist of results from 5556 samples of Jurassic – lowermost Cretaceous shales from 78 wells in the DCG (Table 1). The VR database consists of results from 1175 samples from 55 wells (Table 1) and represents mostly samples of Jurassic age but also includes measurements from younger and older formations.

The quality of the VR measurements is quite variable. The number of VR measurements for each sample

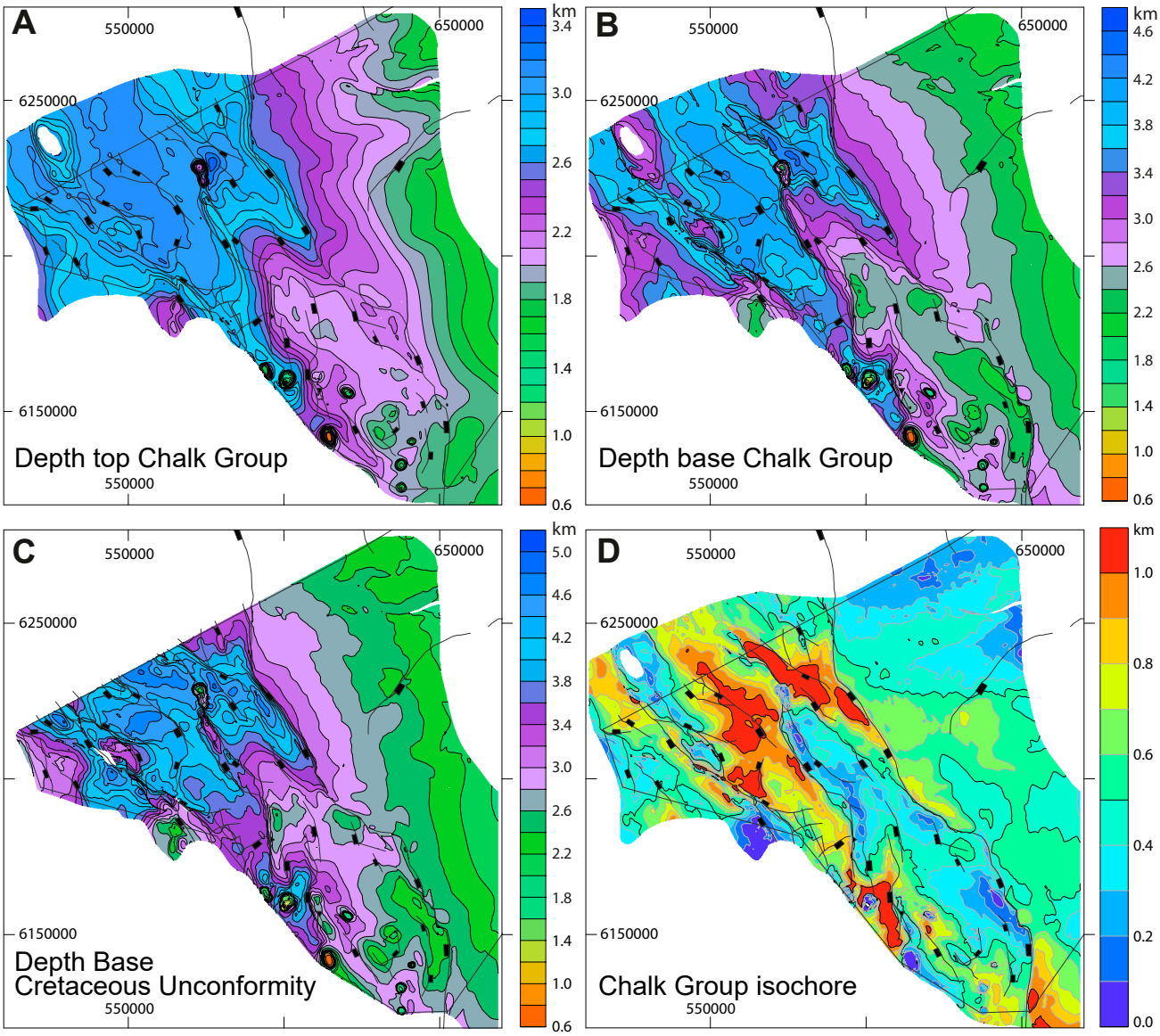

Fig. 5. Depth structure maps and chalk isochore map. **A:** Depth to Top Chalk Group; **B:** Depth to Base Chalk Group; **C:** Depth to Base Cretaceous Unconformity (BCU); **D:** Chalk Group isochore map. Updated from Japsen *et al.* (2003) and Vejbæk *et al.* (2007).

Table 1. Well data included in this work

Well	Area	RE	VR	P	T	1D
A-2X	Salt Dome Province	X			X	
ADDA-1	Salt Dome Province	X			X	
ADDA-2	Salt Dome Province				X	
ALMA-1X	Salt Dome Province	X	X		X	X
ALMA-2X	Salt Dome Province	X			X	
AMALIE-1	Søgne Basin	X	X	X	X	X
ANNE-3	Salt Dome Province	X	X		X	X
BARON-2	Tail End Graben	X	X		X	X
BERTEL-1A	Feda/Gertrud Graben	X	X	X	X	X
BO-1X	Salt Dome Province	X	X		X	X
BOJE-1	Salt Dome Province	X			X	
CLEO-1	Søgne Basin	X	X		X	X
DEEP ADDA-1	Salt Dome Province	X			X	
DIAMANT-1	Feda/Gertrud Graben	X	X		X	X
E-1X	Salt Dome Province	X	X		X	X
EAST ROSA FLANK-1	Salt Dome Province				X	
EAST ROSA-1	Salt Dome Province				X	
EAST ROSA-2	Salt Dome Province				X	
EAST ROSA-3	Salt Dome Province				X	
EDNA-1	Heno Plateau	X	X		X	
EG-1	Heno Plateau	X			X	
ELIN-1	Tail End Graben	X	X	X	X	X
ELLY-1	Heno Plateau	X		X	X	
ELLY-2	Heno Plateau	X	X		X	X
ELLY-3	Heno Plateau	X			X	
ELNA-1	Salt Dome Province				X	
EMMA-1	Salt Dome Province	X		X	X	
FALK-1	Heno Plateau	X	X		X	X
FASAN-1	Salt Dome Province	X	X		X	X
G-1X	Salt Dome Province	X	X		X	X
GERT-1	Feda/Gertrud Graben	X	X	X	X	X
GERT-2	Feda/Gertrud Graben	X	X		X	X
GERT-3	Feda/Gertrud Graben				X	
GERT-4	Feda/Gertrud Graben	X	X			
GITA-1X	Søgne Basin	X	X			
GULNARE-1	Tail End Graben	X	X		X	X
GWEN-2	Feda/Gertrud Graben	X			X	
HEJRE-1	Feda/Gertrud Graben	X	X	X	X	X
HEJRE-2	Feda/Gertrud Graben	X		X	X	
I-1X	Tail End Graben	X	X		X	X
IRIS-1	Tail End Graben	X	X	X	X	X
ISAK-1	Feda/Gertrud Graben	X			X	
JENS-1	Salt Dome Province	X	X	X	X	X
JEPPE-1	Feda/Gertrud Graben	X	X		X	X
JETTE-1	Feda/Gertrud Graben	X			X	
JOHN FLANKE-1	Salt Dome Province	X	X		X	
JOHN-1	Salt Dome Province				X	
KARL-1	Feda/Gertrud Graben	X	X		X	X
KIM-1	Outer Rough	X	X	X	X	X
LILJE-1	Outer Rough	X			X	
LIVA-1	Outer Rough	X			X	
LONE-1	Feda/Gertrud Graben	X	X		X	X
LULITA-1X	Søgne Basin	X	X		X	
LULU-1	Søgne Basin	X	X		X	X
LULU-2	Søgne Basin	X			X	
M-1X	Salt Dome Province				X	
M-8X	Salt Dome Province	X	X		X	X

Table 1 (Continued)

Well	Area	RE	VR	P	T	1D
MIDDLE ROSA-1	Salt Dome Province				X	
MIDDLE ROSA-2	Salt Dome Province				X	
MONA-1	Feda/Gertrud Graben	X	X		X	X
N-22	Salt Dome Province	X			X	
NORA-1	Tail End Graben	X	X	X	X	X
NORTH JENS-1	Salt Dome Province	X	X		X	X
NW ADDA-1X	Salt Dome Province	X		X	X	
O-1X	Salt Dome Province	X	X			X
OLGA-1X	Salt Dome Province	X	X		X	X
OPHELIA-1	Feda/Gertrud Graben	X	X		X	X
OTTO-1	Tail End Graben				X	
P-1X	Outer Rough				X	
PER-1	Salt Dome Province				X	
Q-1X	Feda/Gertrud Graben	X	X		X	X
RAVN-1	Heno Plateau	X	X		X	X
RAVN-2	Heno Plateau	X	X		X	X
RITA-1X	Feda/Gertrud Graben	X	X		X	X
ROBIN-1	Outer Rough	X		X	X	
RUTH-1	Salt Dome Province				X	
S.E. ADDA-1X	Salt Dome Province				X	
S.E. IGOR-1	Salt Dome Province	X	X		X	X
SAXO-1	Outer Rough	X		X	X	
SINE-1XP	Salt Dome Province				X	
SKARV-1	Heno Plateau	X	X		X	X
SKJOLD FLANK-1	Salt Dome Province	X	X	X	X	
STEN-1	Feda/Gertrud Graben	X	X		X	X
STORK-1	Tail End Graben	X	X		X	X
SVANE-1	Tail End Graben	X	X	X	X	X
T-1X	Tail End Graben				X	
T-3X	Tail End Graben				X	
TABITA-1	Tail End Graben	X			X	
TORDENSKJOLD-1	Outer Rough	X	X		X	X
TOVE-1	Salt Dome Province				X	
U-1X	Salt Dome Province	X	X	X	X	X
UGLE-1	Salt Dome Province	X		X	X	
V-1X	Salt Dome Province				X	
VAGN-2	Salt Dome Province				X	
W-1X	Heno Plateau	X	X		X	X
WESSEL-1	Outer Rough	X		X	X	
WEST LULU-1	Søgne Basin	X	X	X	X	
WEST LULU-2	Søgne Basin	X	X		X	
WEST LULU-3	Søgne Basin	X	X		X	
WEST LULU-4	Søgne Basin				X	
XANA-1X	Søgne Basin	X	X	X		X

RE: Rock Eval; VR: Vitrinite reflectance; P: Pressure; T: Temperature; 1D: 1D basin model

varies from 1 to more than 100 and the associated standard deviations typically range between ± 0.02 and 0.11% R_o (Petersen *et al.* 2012). Histograms of the original measurement population are available for most samples, but no re-assessment of the measurements has been made for this study.

A total of 312 down-hole pressure measurements from 22 wells, typically from a repeat formation tester (RFT) tool, and 261 bottom-hole temperature measurements from 97 wells are evaluated here (Table 1). The wells analysed for pressure do not represent all available wells but have been selected based on availability of pressure data in the Jurassic section. The pressure and temperature data are all from drill reports available to the public from GEUS *via* the Frisbee portal (http://frisbee.geus.dk/). The reported pressure data have all been quality controlled and temperature measurements have been 'Horner corrected' according to the correction procedures presented by Waples *et al.* (2004).

Published data in the source rock and VR databases include data previously presented by Thomsen *et al.* (1983), Damtoft *et al.* (1987, 1992), Østfeldt (1987), Petersen & Rosenberg (1998), Petersen *et al.* (1998, 2000, 2010, 2011, 2012, 2013), Petersen & Brekke (2001), Ineson *et al.* (2003) and Ponsaing *et al.* (2018, 2020a,b). Included VR measurements outside of the DCG are from the Norwegian wells 2/11-7, 2/5-9 and 2/12-1 (Petersen *et al.* 2012) that borders on the northern part of the DCG (Fig. 1).

Analytical methods

Both oil- and water-based drilling mud systems have been used in the DCG. Oil-based mud (OBM) systems are known to have a severe impact on data quality if the mud is not properly removed prior to analysis (Petersen *et al.* 2017). In wells drilled using an OBM system, preparative solvent extraction treatment of samples prior to analysis was made. Samples were washed with several batches of dichloromethane until the cuttings appeared clean. The 0.25–4.0 mm size fraction was subsequently recovered by sieving and exhaustively treated by solvent extraction for seven full days using soxhlet instrumentation and a dichloromethane-methanol mixture (93 vol% – 7 vol%) as solvent. In wells drilled using a water-based mud system, cuttings were washed with rinsing tap water. Examination under microscope was made to ensure that the cuttings were completely cleaned.

Since 1992 cuttings for subsequent analysis have been prepared from the 1–4 mm size fraction and ground to less than 0.25 mm for Rock-Eval-type analysis. The selection of this size fraction minimizes the impact of cavings that tend to be larger and rather irregular in shape. For older analyses no specific size fraction was used, but the cuttings are typically from the less than 2 mm size fraction. Samples for VR measurements were not powdered but embedded directly in epoxy.

The TOC content was determined by combustion in a LECO CS-200 induction furnace after elimination of carbonate-bonded carbon by two stages of HCl treatment. In-house and international standards are measured during analysis and the analytical reproducibility is 0.1 wt% TOC. Rock-Eval pyrolysis was carried out using several types of instrumentation. Most data were produced using a Source Rock Analyzer instrument manufactured by Humble Instruments and Services (presently Weatherford). Newer analyses were produced by a HAWK instrument (Wildcat Instruments, USA). Older data were produced by a Rock-Eval 6 instrument or even a Rock-Eval 2 instrument. Calibration was done using the IFP-160000 or IFP-55000 standards, with sets of one blank and one in-house (Marl Slate) control standard being run for every 10 samples to ensure the stability of the instrument. This procedure serves to assure that different generations of data are comparable.

Based on the Rock-Eval pyrolysis, the Hydrogen Index (HI; mg HC/g TOC) was calculated from the S_2 yields in mg HC/g sample by normalising the S_2 yield by TOC ((S_2 /TOC) × 100). T_{max} represents the temperature at which the maximum rate of the hydrocarbon generation (S_2) occurs. The S_1 peak is not considered here due to the mixed dataset of non-extraction-treated and extracted-treated samples.

VR (random) measurements were carried out following standard procedures (Taylor *et al.* 1998). Analysts were all accredited and certified by the International Committee for Coal and Organic Petrology (ICCP). Since 2011 measurements were conducted using a Leitz Orthoplan reflected-light microscope equipped with a 50× oil objective and the Diskus Fossil System (Hilgers Technisches Büro). VR readings were taken at 546 nm (monochromatic light) and before measurement the microscope was calibrated against a YAG 0.903% R_o standard with integrated optical zero standard. The number of measurements in each sample varied depending on lithology and organic-richness (TOC content) but in general at least 20 measurements were made.

Statistical and regression analysis

For the analysed formations the TOC, HI and T_{max} frequency distributions are skewed, and representative statistical properties cannot be calculated by assuming a normal distribution. Instead, to provide the best descriptive statistical properties, modelling of the cumulative density frequencies were made assuming a log-normal distribution. Fitting was made with the SigmaPlot® version 14 from Systat Software, which allows iterative modelling to be made in order to obtain the mean and standard deviation of the log-normal distribution. The match of the data and model was evaluated from the goodness of fit (r^2). All accepted models had $r^2 > 0.98$. Based on the obtained mean and standard deviation of the log-normal distribution the population mean, standard deviation, and various percentiles (P) of the population were calculated using standard procedures.

The Partial Least Squares (PLS) multivariate regression method was used to examine relationships between VR and depth with respect to the sea floor, top Chalk Group, base Chalk Group and the Base Cretaceous Unconformity in order to develop predictive models. The PLS regression allows direct correlations to be modelled between y and the multivariate x data, compensating for debilitating co-linearity between

x-variables (Esbensen & Swarbrich 2018). A PLS regression model depends on proper validation, which is here based on a test set prepared before modelling by randomly splitting the data into two independent data sets, i.e. the training versus the test set, securing a realistic prediction performance validation (Esbensen & Geladi 2010; Esbensen & Swarbrich 2018). All data were auto-scaled by subtracting the average and dividing with the standard deviation and the modelling was performed in the software package Unscrambler® 10.5 by CAMO.

Basin modelling

Basin modelling was made with the PetroMod® software (Integrated Exploration Systems GmbH, Aachen, Germany; v2015.2). The software is used for integration of geological, geophysical, geochemical and petrophysical data and for testing hypotheses regrading origin and evolution of the petroleum resources. In such models the thermal maturity of the source rock succession is crucial when the timing and extent of source rock maturation is assessed (see e.g. Magoon & Dow 1994 for case studies).

The main object of the basin modelling in this study was to examine the maturity using 1-D basin maturity modelling on 46 wells (Table 1) and four pseudo-wells. Based on the 'most likely' input parameters the regional maturity trend and the position relative to the oil window was investigated, where the oil window is defined as VR between 0.55 and 1.3% R_o, and the gas window as VR between 1.3 and 4.0% R_o. However, in the DCG the oil window for a Type II kerogen is believed to correspond to what in PetroMod is called 'Main oil', i.e. the 0.7–1.0% R_o interval. The 1-D models use a tectonic-stratigraphic framework allowing the 1-D PetroMod to quantify all important basin processes as a function of time, including thermal history calibration based on VR and temperature measurements. Event-splitting of the Upper Jurassic – lowermost Cretaceous successions is based on a sequence stratigraphic framework (Fig. 3). The Lower Cretaceous is treated as one event, i.e. the Cromer Knoll Group, while the Chalk Group is divided into two events. The post Chalk Group is subdivided into 11 Palaeogene – Neogene events based on maps published by Rasmussen *et al.* (2005) and three Pleistocene events based on in-house (GEUS) subdivisions. The adapted modelling concept was adjusted for the Farsund Formation by applying the Pepper & Corvi (1995) organofacies classification. Absolute ages for the Mesozoic are based on Gradstein *et al.* (2012, 2014) and absolute ages for the post Chalk Group strata are based on unpublished GEUS data.

The PetroMod standard lithofacies library was used and is based on adapted information on depositional facies variation and other available information. The boundary conditions are palaeo-water-depth, sediment–water-interface temperature and basal heat flow. The boundary conditions define the basic energetic conditions for the temperature development for all layers, especially the source rock intervals and, consequently, the maturation of organic matter through time. The palaeo-water-depths through time were constructed using information on depositional settings, palaeo-environmental information from wells and sediment thickness maps.

Results

The analysed wells in the DCG are grouped into six areas with a basin development as internally similar as possible in order to illustrate the differences in source quality and maturity in the DCG (Japsen *et al.* 2003; Møller & Rasmussen 2003; Rasmussen *et al.* 2005). With reference to structural elements presented in Fig. 1 the areas are: 1) the Salt Dome Province including the Rosa Basin and Poul Plateau, 2) the Tail End Graben including the Arne-Elin Graben, 3) the Feda Graben, the Gertrud Plateau and Graben including the Inge High and the Lindesnes and Gert ridges, 4) the Søgne Basin, 5) the Heno Plateau and 6) the Outer Rough Basin including the Ål Basin and the Mid North Sea High and Robin High (Fig. 6A). For some wells (see Table 1), the division between the areas are somewhat arbitrary depending on emphasis of the Jurassic or the Cretaceous development. This includes the Diamant-1, Gwen-2, Jette-1 and Q-1 wells, which are assumed to represent the Feda–Gertrud Graben.

Source rock quality and T_{max} variation within the Danish Central Graben

Within each of the six areas outlined above (Fig. 6A), the source rock quality and maturity for the following formations are presented below (see Fig. 3 for stratigraphy):

1) The Lower Jurassic (Hettangian – Pliensbachian) marine Fjerritslev Formation.
2) The Middle Jurassic to lowermost Upper Jurassic (Aalenian – Oxfordian) floodplain to estuarine Bryne, Lulu and Middle Graben Formations (hereafter treated together as 'Middle Jurassic source rocks').
3) The Upper Jurassic (Oxfordian – Kimmeridgian) marine Lola Formation.
4) The Upper Jurassic to lowermost Cretaceous (Kimmeridgian – Ryazanian) marine Farsund Formation.

For the Farsund Formation, the source rock data are also tabulated for specific stratigraphic intervals including the Volg-1, the Volg-4 and the Ryaz-1 sequences (Fig. 3), as these sequences are known to have better source rock qualities than the general quality in the remaining part of the succession (Ineson *et al.* 2003; Petersen *et al.* 2010, 2017; Ponsaing *et al.* 2018, 2020a,b).

The population statistics have been calculated assuming a log-normal distribution that has been fitted to the cumulative frequency distributions as shown in Fig. 6B. The source rock characteristics for each formation are presented as histograms for each of the six areas in Fig. 7 and as population statistical parameters (mean, median (P50), low (P90) and high (P10)) in Table 2.

The source-rock richness is evaluated from a combination of TOC content and HI with respect to the present-day maturity as indicated by the T_{max}. The nomenclature follows Peters (1986); for shales with dominantly marine kerogen, TOC below 0.5 wt% is considered poor, 0.5–1.0 wt% fair, 1.0–2.0 wt% good and above 2.0 wt% very good. For evaluation of the generative potential we use the HI (evaluated from immature sample); HI below 150 mg HC/g TOC is considered gas-prone; 150–300 mg HC/g TOC mixed oil/gas-prone and above 300 mg HC/g TOC oil-prone. The onset of the oil window is assumed to be at a T_{max} between 435 and 445°C (equivalent of 0.6% R_o) and the end of the oil window is assumed to be at a T_{max} of 470°C (equivalent of 1.4% R_o). However, matured source rocks will have their TOC and HI lowered due to generation of hydrocarbons and thus this approach inherits a weakness in assessing mature to over-mature samples. Likewise, many maturity parameters, and particularly T_{max}, depend on the kerogen type and thus the onset of the oil window is not necessarily the same for all formations.

Fjerritslev Formation

The Fjerritslev Formation was originally defined in the Danish Basin where its maturity and source rock properties are well described (Thomsen *et al.* 1987; Petersen *et al.* 2008). In the DCG the formation is known only as erosional remnants due to extensive mid-Jurassic erosion. Maximum thickness drilled is 257 m found in the Edna-1 well (Michelsen *et al.* 2003). The formation is dominated by dark grey, slightly calcareous shales with the lower parts being more calcareous and silty (Michelsen *et al.* 2003). The Fjerritslev Formation has been drilled and analysed in both the Salt Dome Province and on the Heno Plateau (Fig. 7). The unit is probably present also in the Tail End Graben but has not been drilled (Fig. 4A).

The TOC content and source rock properties on the Heno Plateau (the Edna-1 and Skarv-1 wells) are good with an average TOC of 1.3 wt% (median 1.3

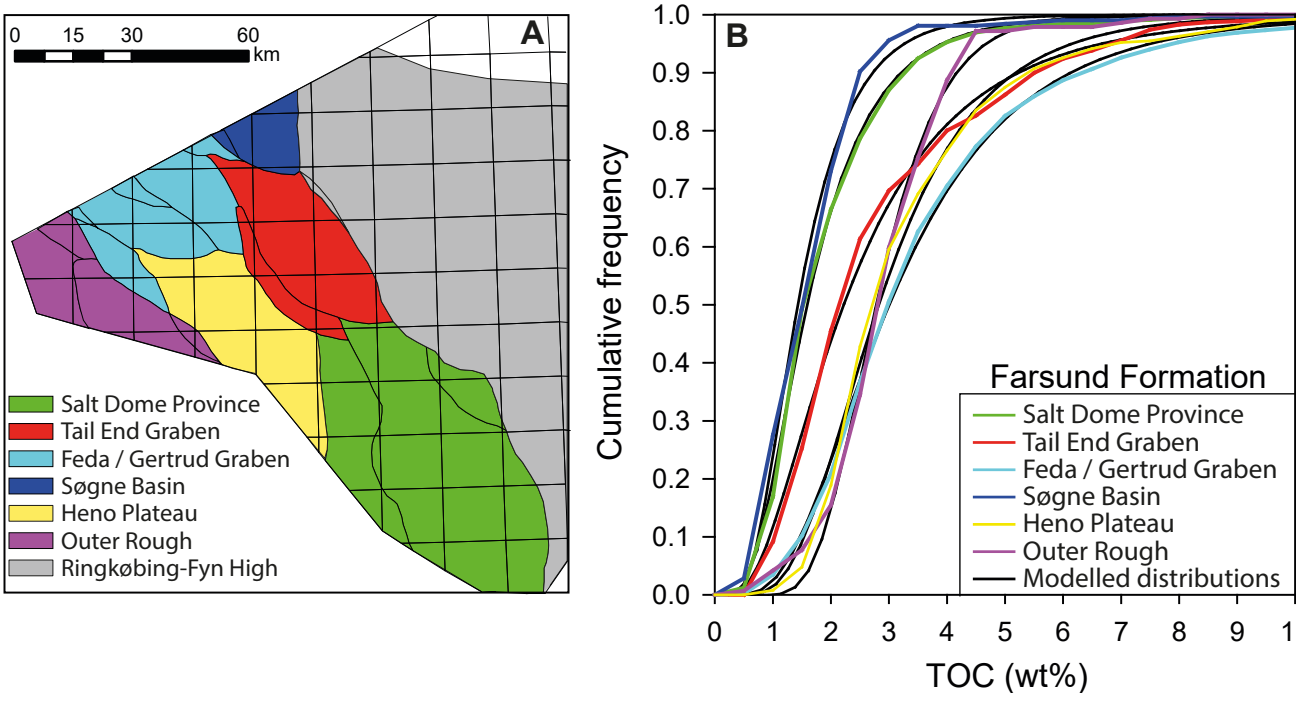

Fig. 6. A: Semi-regional structural subdivision of the Danish Central Graben; **B**: Cumulative frequency of the TOC content in the Farsund Formation within the six areas of the Danish Central Graben. Data are presented in Figs 7–9. Each cumulative frequency distribution has been modelled using a log-normal model (black lines) and their means and standard deviations are presented in Table 2.

Table 2. Source rock characteristics of Jurassic – lowermost Cretaceous formations and selected sequences in the Farsund Formation

Area	Formation / sequence	TOC (wt%)				HI (mg HC/g TOC)				T_{max} (°C)			
		Mean	P90	P50	P10	Mean	P90	P50	P10	Mean	P90	P50	P10
Salt Dome Province													
	Farsund Formation	1.8	0.8	1.6	3.2	231	186	228	280	431	426	431	436
	Ryaz-1	3.6	1.7	3.2	6.0	364	213	341	546	428	422	428	433
	Volg-4	1.9	1.0	1.7	2.9	222	102	195	374	430	427	430	433
	Volg-1	1.9	1.0	1.7	2.9	189	85	165	322	432	428	432	435
	Farsund other*	1.7	0.8	1.5	2.8	178	83	157	298	431	427	431	436
	Lola Formation	1.5	0.9	1.4	2.1	138	82	130	205	434	427	434	441
	Bryne/Lulu/M.G. Formations	3.3	1.1	2.6	6.2	94	54	88	142	439	428	439	450
	Fjerritslev Formation	2.1	1.2	2.0	3.2	Bimodal distribution				436	428	436	444
Tail End Graben													
	Farsund Formation	2.8	0.9	2.2	5.2	171	63	141	313	439	433	439	445
	Ryaz-1	4.7	2.2	4.1	7.8	283	156	261	437	438	434	438	442
	Volg-4	2.4	1.0	2.0	4.2	180	80	157	308	439	436	439	443
	Volg-1	1.8	1.1	1.7	2.6	119	49	102	211	443	433	443	453
	Farsund other*	2.2	1.0	1.9	3.8	128	64	115	208	439	431	439	447
	Lola Formation	1.2	0.2	0.7	2.7	104	48	92	175	434	424	434	445
	Bryne/Lulu/M.G. Formations	1.4	0.5	1.2	2.7	55	22	47	98	not defined			
Feda and Gertrud Grabens													
	Farsund Formation	3.5	1.5	3.0	6.1	238	106	207	405	439	433	439	445
	Ryaz-1	5.0	2.2	4.3	8.5	369	223	347	542	439	434	439	444
	Volg-4	3.2	1.4	2.8	5.6	249	127	226	401	440	435	440	445
	Volg-1	3.2	1.5	2.9	5.3	232	91	194	415	440	433	440	446
	Farsund other*	3.4	1.5	3.0	5.9	212	104	189	346	439	432	439	445
	Lola Formation	2.0	0.6	1.5	3.8	168	85	152	270	440	430	440	450
Søgne Basin													
	Farsund Fm	1.6	0.8	1.4	2.7	161	63	135	290	437	430	437	443
	Farsund other*	1.6	0.8	1.4	2.7	156	63	132	277	437	430	437	443
	Lola Fm	1.8	1.0	1.7	2.9	144	78	133	225	438	431	438	444
	Bryne/Lulu/M.G. Fms (TOC< 20%)	3.5	0.7	2.2	7.6	171	99	160	256	444	436	444	452
	Bryne/Lulu/M.G. Fms (TOC> 20%)	69.6	51.7	69.6	87.4								
Heno Plateau													
	Farsund Formation	3.2	1.5	2.8	5.2	207	94	181	351	438	434	438	442
	Ryaz-1	5.6	1.8	4.4	10.6	379	180	336	628	435	432	435	439
	Volg-4	4.9	2.8	4.6	7.6	238	133	220	364	438	435	438	442
	Volg-1	3.5	1.8	3.2	5.8	193	86	168	329	439	435	439	442
	Farsund other*	2.7	1.6	2.5	3.9	178	93	162	283	439	435	439	442
	Lola Formation	2.1	0.8	1.7	3.8	161	84	146	256	439	431	439	447
	Fjerritslev Formation	1.3	1.0	1.3	1.7	64	35	59	98	447	435	447	459
Outer Rough													
	Farsund Formation	2.9	1.9	2.8	4.2	213	77	174	393	441	432	441	450
	Volg-4	3.3	2.6	3.3	4.2	235	108	207	397	439	432	439	446
	Farsund other*	2.7	1.6	2.5	3.9	199	63	155	383	442	433	442	451

*Excluding Volg-1, Volg-4 and Ryaz-1. M.G.: Middle Graben Formation. P10 indicates the value that 10% of the population will exceed; P50 indicates the median of the population; P90 indicates the value that 90% of the population will exceed. Calculated based on modelled log-normal distributions. For wells included, see Table 1.

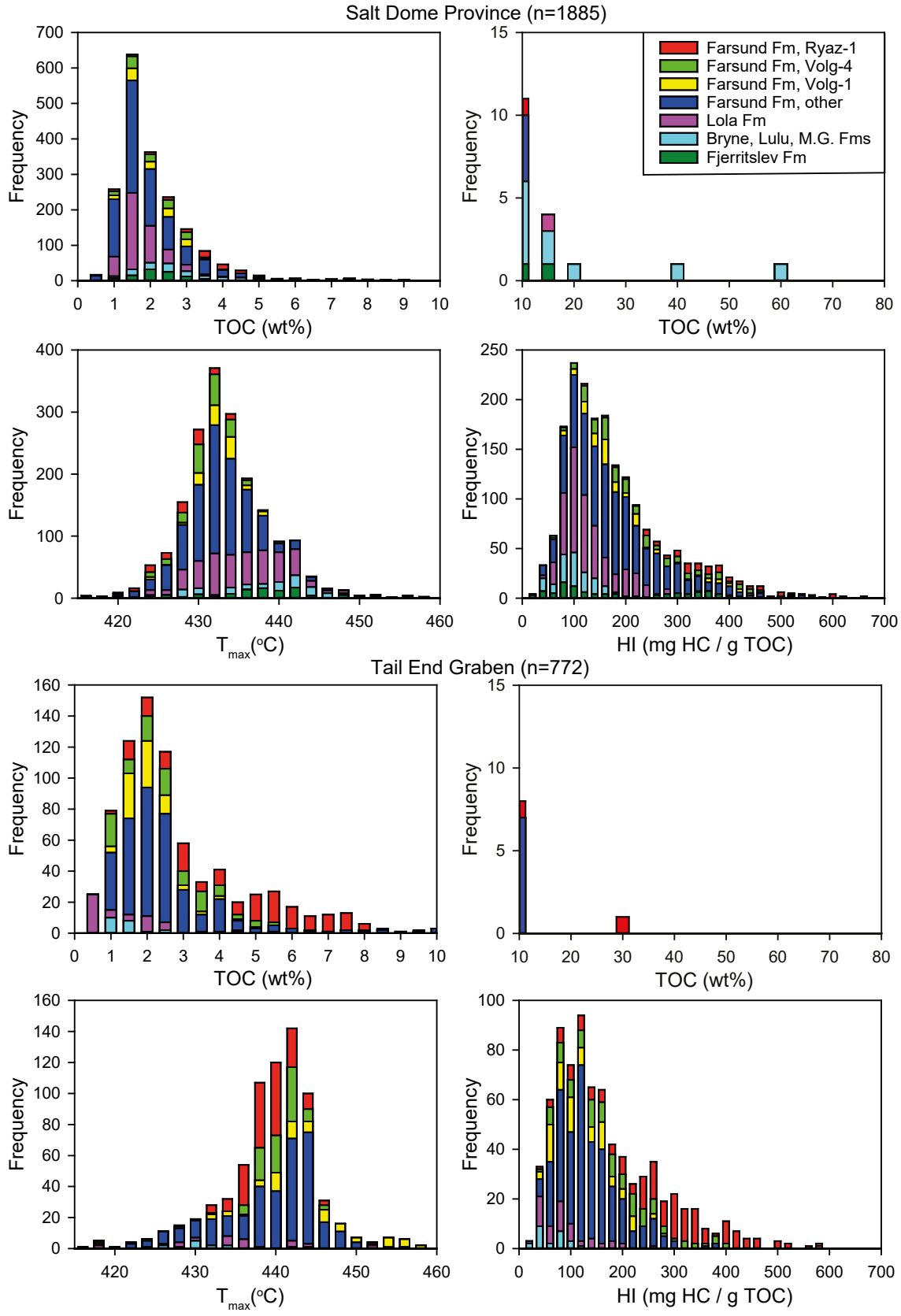

Fig. 7. Histograms of present-day TOC, T_{max} and present-day HI within six areas of the Danish Central Graben. For wells included, see Table 1. For area subdivision, see Fig. 6A. Note that the histogram for TOC is displayed for TOC < 10 wt% and for TOC > 10 wt%. Farsund other: The Farsund Formation with contributions from the Volg-1, Volg-4 and Ryaz-1 sequences excluded.

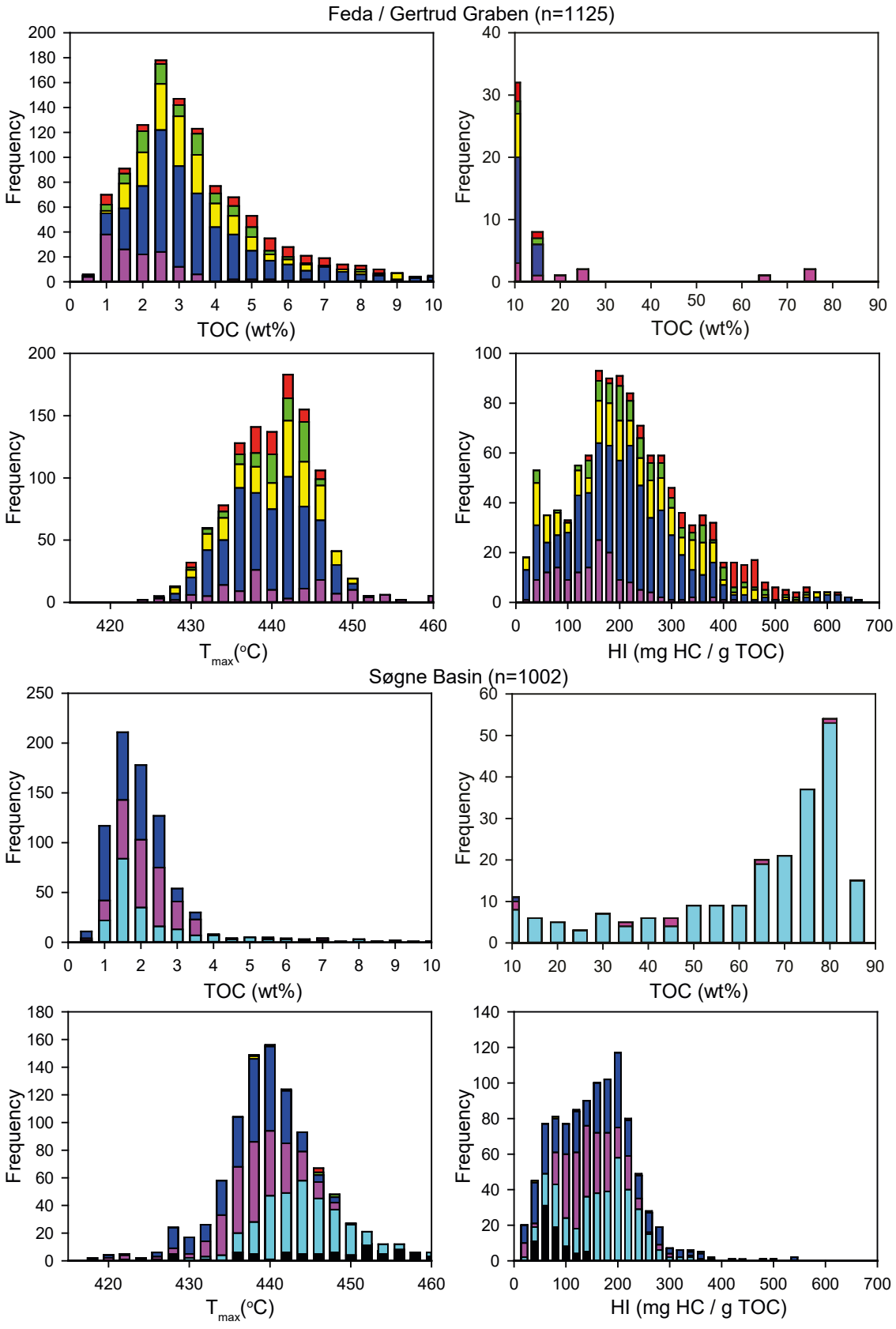

Fig. 7 (Continued).

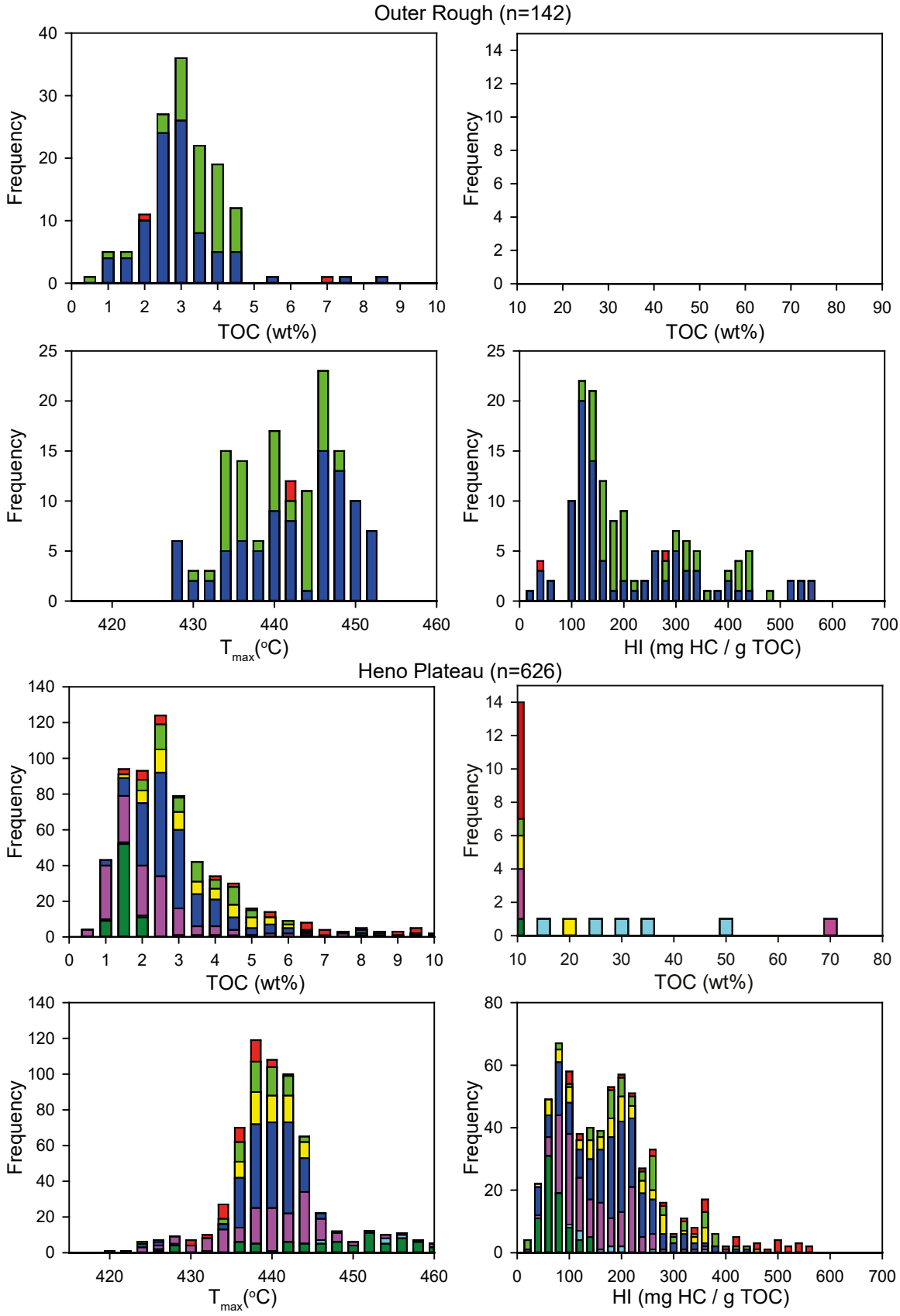

Fig. 7 (Continued).

wt%). The average HI is 64 mg HC/g TOC but as the formation is mature (average T_{max} 447°C), this hampers direct evaluation of the generation potential. In the Salt Dome Province (the Jens-1, John Flanke-1, M-8X, N-22X, Olga-1X, O-1X and U-1X wells), the formation attains better source rock properties with average TOC values of 2.1 wt% (median 2.0 wt%). The formation is immature (average T_{max} 436°C). The HI distribution is, however, bimodal and no meaningful formation average can be calculated. The formation includes oil-prone beds as the HI ranges up to more than 400 mg HC/g TOC (Fig. 7). As the measurements were made on extraction-treated cuttings samples, these high HI values are assumed to reflect the kerogen composition of the rock. A mixed oil/gas generative potential is thus assumed for the formation.

Middle Jurassic source rocks

The Bryne, Lulu and Central Graben Formations are treated here as one unit with respect to the source rock evaluation. Of these formations, the source rock quality of the coals and coaly shales of the Bryne and Lulu Formations have recently been reviewed by Petersen & Hertle (2018) for the Harald-Lulita-Trym area (Fig. 1, the West Lulu-1, -2, -3, Lulu-1, Lulita-1 and 3/7-4 wells), and we refer to this publication for specific details on the occurrence in this area.

The Middle Jurassic succession may attain thickness up to several hundred metres and include marine to paralic sandstones interbedded with coaly claystone, and also coal seams up to 5 m in thickness (Michelsen *et al.* 2003; Andsbjerg & Dybkjær 2003; Petersen & Hertle 2018). Deposition took place in a variety of environments including fluvial, floodplain, lacustrine and estuarine (Fig. 4B). The Middle Jurassic source rocks have been sampled in all areas except for the Feda and Gertrud Grabens and the Outer Rough Basin. Except for the Søgne Basin, the samples generally have less than 20 wt% TOC (Fig. 7) and represent rather thin coaly beds or sediments with disseminated coal. The kerogen type is dominantly terrestrial and the average TOC is in the range 1.4–3.3 wt% with the lowest values measured in the Tail End Graben. Here only 24 samples are available from the Nora-1 well. Because of this, no population statistics could be established for the T_{max} (Table 2). In the Søgne Basin, a bimodal TOC distribution is seen. For samples with less than 20 wt% TOC the average content is 2.2 wt%, and for samples with TOC above 20 wt% the average content is 69.6 wt%. The average HI of the Middle Jurassic source rocks is in the range 55–171 mg HC/g TOC with the highest values measured in the Søgne Basin (T_{max} 444°C). Restoring the source rock to its original HI values (pre-generative level) suggests that these were around 270 mg HC/g TOC with even higher values for proximal lacustrine deposits (Petersen & Hertle 2018), indicating an original mixed oil/gas to oil generative potential as documented by liquid–source rock correlations (Petersen *et al.* 1996, 2000).

Lola Formation

The Lola Formation is present in the eastern and southern parts of the DCG where it may attain a thickness of *c.* 1 km (Michelsen *et al.* 2003). The formation consists of dark olive-grey to grey shales deposited in a low-energy offshore open marine environment. The average TOC content is fair to good as it varies between 1.2 and 2.1 wt% (median 0.7–1.7 wt%), with the highest concentrations reached on the Heno Plateau and the lowest in the Tail End Graben (Table 2). The average HI in the immature Salt Dome Province (average T_{max} 434°C) is 138 mg HC/g TOC, suggesting a gas-prone nature of the kerogen, which agrees with previous assessments (Michelsen *et al.* 2003; Ponsaing *et al.* 2018).

Farsund Formation

The Farsund Formation is present throughout the DCG and correlates partially with the Kimmeridge Clay Formation and the Mandal Formation in the UK and Norwegian Central Graben (Michelsen *et al.* 2003; Petersen *et al.* 2010, 2013; Verreussel *et al.* 2018). The thickness of the succession may exceed 3 km in the Tail End Graben. The Farsund Formation consists of medium grey to dark shale with numerous thin beds of brownish dolomite. Deposition took place in a relatively deep marine environment, and sandstones only occur either as turbidites or as gravity flow deposits, especially towards the deeper parts of the basin (Fig. 4C).

Within the uppermost of the Jurassic to lowermost Cretaceous sequences (Volg-4 to Ryaz-1 sequences, Fig. 3) of the Farsund Formation, a unit with a conspicuously high gamma ray response occurs, the Bo Member (in older literature the 'Hot Unit', Michelsen *et al.* 2003). The member is present throughout the DCG although it is typically absent (eroded) on structural highs. Thicknesses vary from less than 10 m in the Salt Dome Province to more than 100 m in the Tail End Graben (Ineson *et al.* 2003). The Bo Member is dominated by black to dark-brown laminated organic-rich claystone deposited in a low-energy oxygen-deficient environment (Michelsen *et al.* 2003).

For the entire Farsund Formation the average TOC ranges from good to very good (average 1.8–3.5 wt%, median 1.4–3.0 wt%) with the lowest values in the Søgne Basin and the highest values in the Feda and Gertrud Grabens (Table 2). The average HI of the Farsund Formation in the immature Salt Dome Province is 231 mg HC/g TOC, suggesting an overall mixed oil/

gas generative potential, which agrees with previous assessments for this area (Damtoft *et al.* 1987, 1992; Petersen *et al.* 2012).

The lowermost Cretaceous (Ryaz-1 sequence) part of the formation has very good TOC values (TOC average 3.6–5.6 wt%, median 3.2–4.4 wt%) with highest values reached on the Heno Plateau and lowest values in the Salt Dome Province (no occurrence in the Søgne Basin and Outer Rough Basin). The HI in the immature Salt Dome Province (average T_{max} 428°C) is 364 mg HC/g TOC, suggesting oil-prone kerogen. A high average HI index (369–379 mg HC/g TOC) also characterises the interval in the early mature Feda and Gertrud Grabens (average T_{max} 439°C) and the Heno Plateau (average T_{max} 435°C). On the Heno Plateau the HI ranges up to 628 mg HC/g TOC (P10), suggesting that the HI was initially richer in this area and thus that a considerable regional variability in the oil richness exist. On the Heno Plateau the TOC ranges up to 13 wt% (P05, Fig. 8).

The Volg-4 sequence shows almost the same overall source-rock richness on the Heno Plateau as the Ryaz-1 sequence, but for other areas the Ryaz-1 sequence richness is not matched by the Volg-4 sequence (Fig.

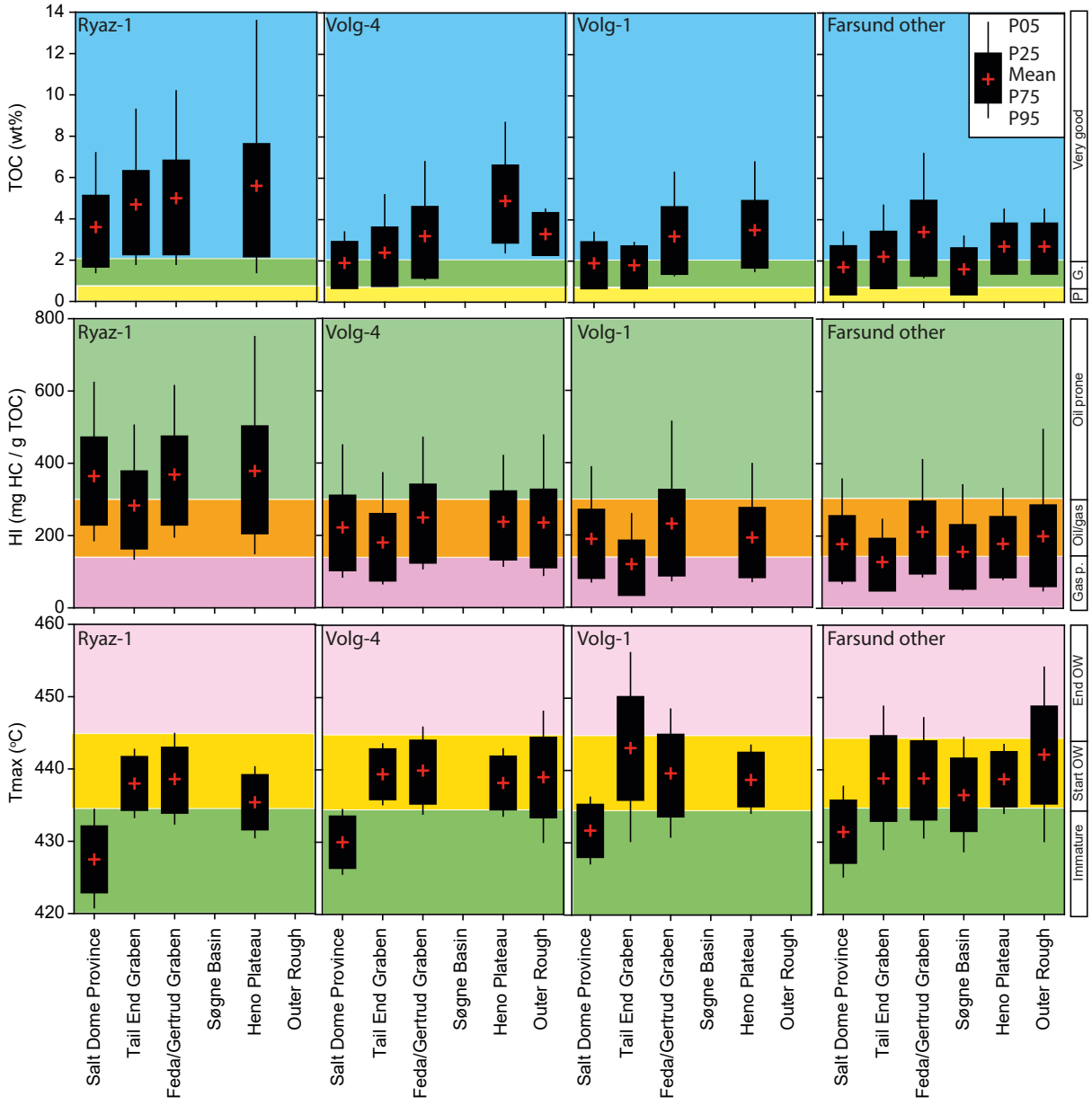

Fig. 8. Box plot (mean, P95, P75, P50, P25 and P05) for the TOC, T_{max} and HI populations within the Farsund Formation and selected sequences. The percentile (P) of the distributions are calculated based on Table 2. Abbreviations: P: Poor; G: Good; Gas p.: Gas prone; Oil/gas: Oil/gas prone; OW: Oil Window.

8). In general, the Volg-4 sequence interval ranges between good and very good TOC values (mean 1.9–4.9 wt%, median 1.7–4.6 wt%). The lowest TOC content is measured in the Salt Dome Province where it is very close to the average value of the Farsund Formation. The HI in the immature Salt Dome Province suggest a mixed oil/gas-prone generative potential (average 222 mg HC/g TOC). However, the HI in the more mature parts of the DCG is similar to that of the immature Salt Dome Province, suggesting an initially unequal distribution in oil richness within the DCG.

For the Volg-1 sequence, only the Feda and Gertrud Grabens and the Heno Plateau have very good TOC contents (average 3.2–3.5 wt%, median 2.9–3.2 wt%). Elsewhere, the interval has only good TOC levels in the Tail End Graben (mean 1.8 wt%). In the immature Salt Dome Province, the average HI is only 189 mg HC/g TOC, suggesting a rather limited oil generating potential. In the mature and TOC-rich Feda and Gertrud Grabens and the Heno Plateau, the average HI is in the range 193–232 mg HC/g TOC, suggesting a higher initial oil generative potential in these areas compared to the Salt Dome Province (Fig. 8, Table 2).

In the Farsund Formation excluding the Volg-1, Volg-4 and Ryaz-1 sequences ('Farsund other' in Fig. 8 and Table 2), the average TOC content varies from 1.6 to 3.4 wt% with the lowest value measured in the Søgne Basin and the highest value measured in the

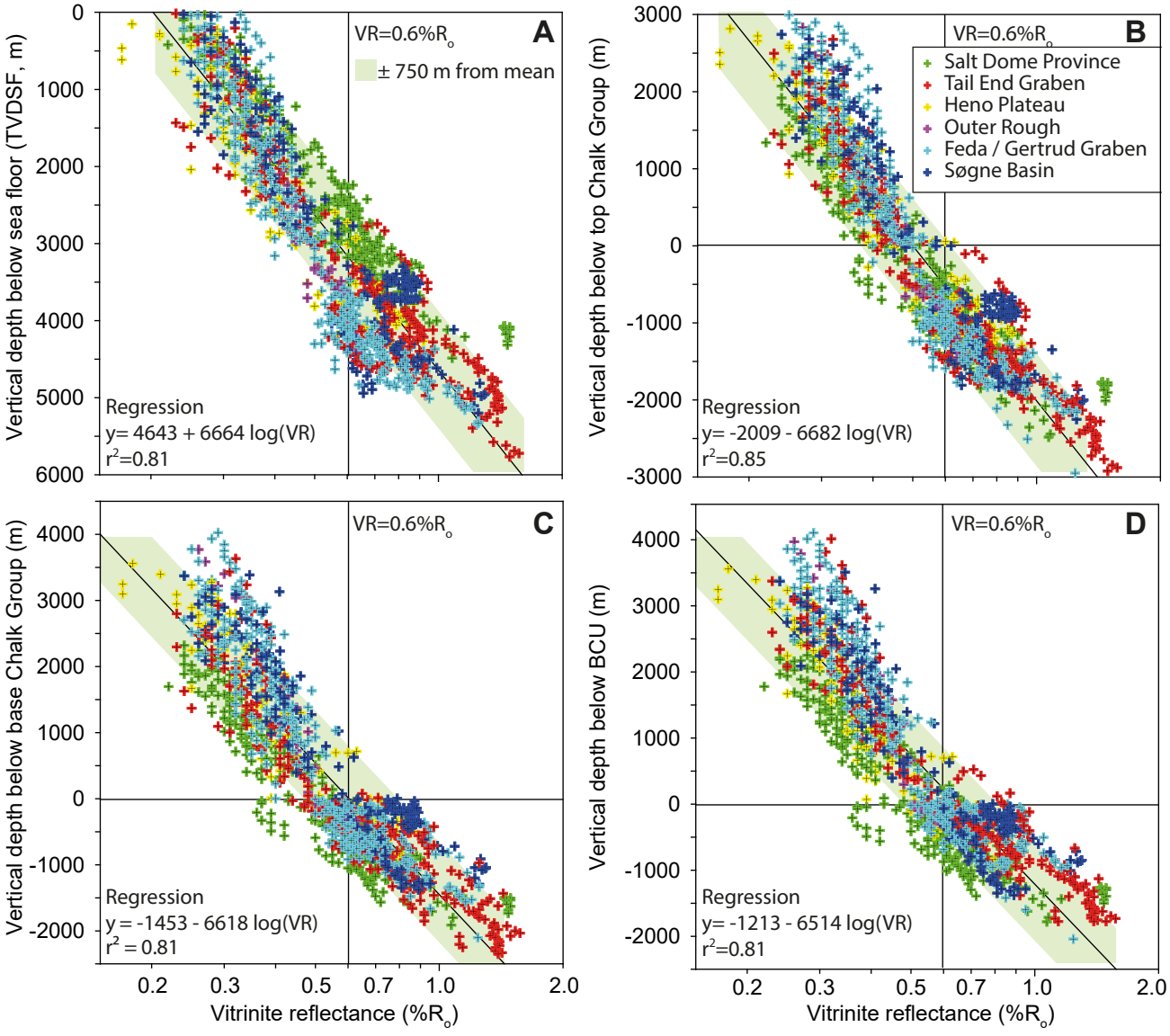

Fig. 9. Vitrinite reflectance (VR) versus depth. **A:** Below present-day sea floor; **B:** Below the top Chalk Group; **C:** Below the base Chalk Group; **D:** Below the base Cretaceous Unconformity (BCU). For reference, the R_o = 0.6% (earliest oil window) is shown. Depths below reference level in B, C, and D are shown as negative.

Feda and Gertrud Grabens (Table 2). The second-lowest TOC content is from the immature Salt Dome Province. Here the average HI is 178 mg HC/g TOC, indicative of a mixed oil/gas generative potential.

Vitrinite reflectance

A total of 1175 samples from 55 wells have been analysed (Table 1). The VR measurements exhibit a strong, statistically significant ($r^2 = 0.81$, n = 1175) linear increase with depth when plotted on a semi-logarithmic scale as is by custom done for this type of data (Fig. 9). Based on the relation in Fig. 9A, a regional model for the DCG can be established according to equation 1:

Regional VR-model:

$$VR\ (\%\ R_o) = 10^{(0.000122 \cdot depth - 0.617)} \quad (1)$$

where depth is measured vertically in metres below sea floor.

The VR slope intercepts at sea floor between 0.1 and 0.25% R_o as expected for non-uplifted basins (see also Petersen *et al.* 2017). There is, however, a considerable spread around the correlation line amounting to about 1500 m (±750 m) for each R_o value (Fig. 9A). For the VR interval corresponding to the earliest oil window and to the middle oil window (0.6–0.8% R_o), the range in depth is even higher. The depth range for a VR measurement of 0.6% R_o is thus 2200–4500 m (Fig. 9A). In general terms, the shallowest depths occur in the Salt Dome Province (the Bo-1X and M-8X wells) and the deepest in the Søgne Basin (Gita-1 well) and the Feda and Gertrud Grabens (Jeppe-1 well).

The depth range of the 0.6–0.8% R_o interval is reduced somewhat if the sample depth is plotted with reference to the top Chalk Group, the base of the Chalk Group or the BCU (Fig. 9B–D). This suggests that the depth of the oil window reflects differences in the subsidence history, notably the depth of the top and base of the Chalk Group. It also appears that the top of the Chalk Group is immature to slightly mature, as the range in VR for the top of the Chalk Group is 0.3–0.6% R_o (Fig. 9B). In a similar manner, the base of the Chalk Group is observed typically to be within the oil window (0.4–0.8% R_o, Fig. 9C).

For the BCU level, the range in VR is 0.4–1.0% R_o with the lowest measured in the Salt Dome Province and the highest in the Tail End Graben (Fig. 9D). The depth range of the oil window (i.e. 0.6% R_o) suggests that it lies up to 1000 m below the BCU in the Salt Dome Province, whereas for the remaining areas,

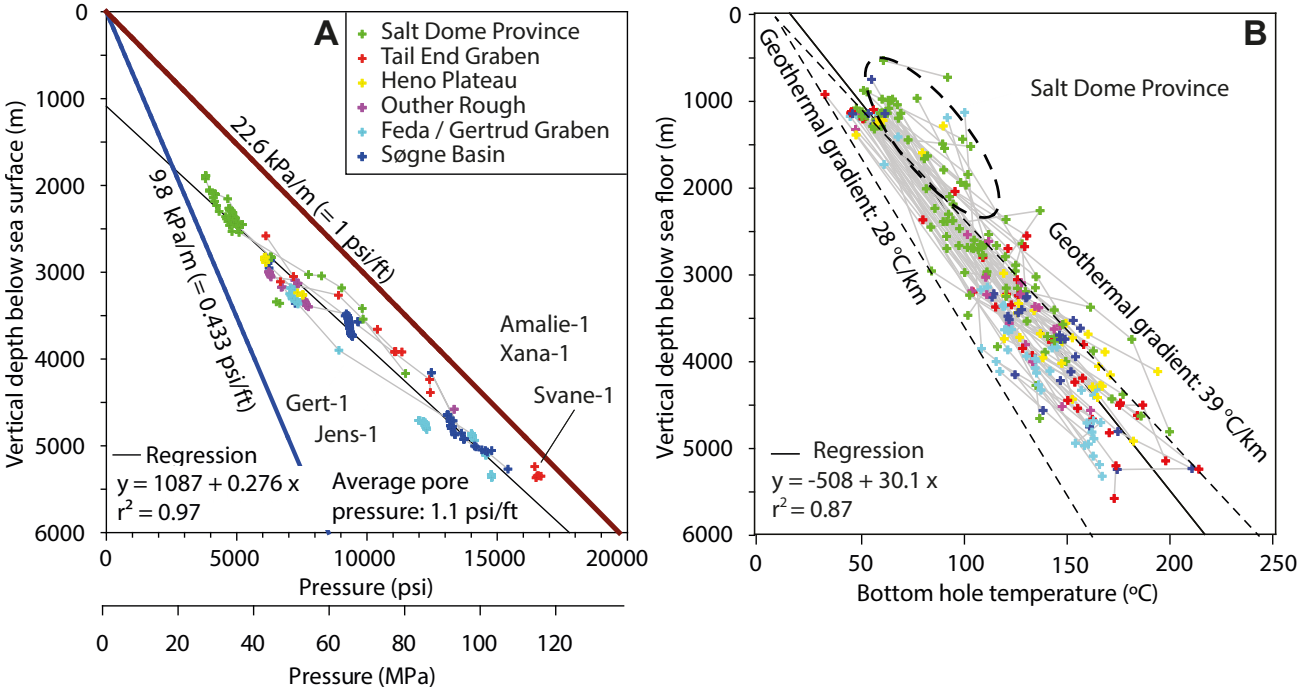

Fig. 10. A: Down-hole fluid pressure measurements versus depth below sea surface. Hydrostatic pressure (9.79 kPa/m, equal to 0.433 psi/ft) and lithostatic pressure (22.6 kPa/m, equal to 1 psi/ft) gradients are shown assuming a water density of 1.0 g/cm³ and an average rock density of 2.3 g/cm³. **B:** Bottom-hole temperatures corrected for environmental conditions according to Waples *et al.* (2004) versus depth below sea floor. Temperature gradients assuming 28°C/km and 39°C/Km and sea floor temperature of 8°C are shown. Broken curve encircles particularly high temperatures measured in wells in the Salt Dome Province. Grey lines connect measurements within the same well. For wells included see Table 1.

the top of the oil window lies either slightly above or within the topmost 200 m of the Jurassic interval (Fig. 9D).

Fluid pressure and down-hole temperature

The pressure versus depth trend of 312 measurements from 22 wells (Table 1) in the DCG is presented in Fig. 10A. The fluid pressure measurements exhibit a linear increase with depth ($r^2 = 0.97$, n = 312) (Fig. 10A) with a pressure versus depth trend described by:

$$\text{Pressure (MPa)} = 24.9\ \text{kPa/m} \cdot \text{depth} - 27.2\ \text{MPa} \quad (2)$$

where depth is measured vertically below sea surface in kilometres.

As expected, the measurements are enclosed by the hydrostatic pressure gradient (9.8 kPa/m) that represents a water density of 1.0 g/cm^3, and the lithostatic pressure gradient (22.6 kPa/m) that represents a rock density of 2.3 g/cm^3 (Fig. 10A). Within the reservoirs, the fluid pressure measurements follow the hydrostatic gradient, whereas the occurrence of pressure seals leads to more rapid increases in pressure than expected from the hydrostatic gradient. The pressure versus depth profiles have been shown in great detail by Petersen *et al.* (2012) for wells in the northern part of the DCG. In our data these features are clearly identified in all of the areas in the DCG as exemplified by the Gert-1 (Feda/Gertrud Graben) and the Jens-1 (Salt Dome Province) wells. Samples from the shallowest part of the wells follow the hydrostatic trend whereas samples in the deeper parts are offset to higher pressures (Fig. 10A). At depths of more than 3 km all wells follow the same overall pressure level, suggesting that all basin areas attain the same high pressure at depths, being just 10% lower than the lithostatic pressure predicts (Fig. 10A).

The bottom-hole temperature versus depth relationships were examined in 97 wells in the DCG (Table 1, Fig. 10B). The temperature exhibits a strong linear increase ($r^2 = 0.87$, n = 261) that follows equation 3:

$$\text{Bottom-hole temperature (°C)} = 33.2\text{°C/km} \cdot \text{depth} + 16.9\text{°C} \quad (3)$$

where depth is measured vertically below the sea floor in kilometres.

Assuming an average sea floor temperature of 8°C, the bulk of the temperature measurements can be confined between a low geothermal gradient of 28°C/km and a high geothermal gradient of 39°C/km as shown in Fig. 10B. These gradients are well within the range of geothermal gradients in the North Sea (Kubala *et al.* 2003). At depths of more than 3 km the bottom hole temperatures from wells in the Feda and Gertrud Grabens tend to cluster at low temperatures (Fig. 10B), suggesting that these areas are relative cold compared to other areas in the DCG. One particular group of relatively shallow samples from the Salt Dome Province (samples from 1–2 km depth in Fig. 10B) appear to be much warmer than predicted from a geothermal gradient of 39°C and thus suggest that this part of the DCG received an extraordinary heat contribution. For the Central Graben it is generally known that the presence of salt imparts a higher conductivity to the section as a whole and elevates the gradients in shallow strata (Kubala *et al.* 2003), and we suspect that this is what is seen in Fig. 10B.

As part of the 1-D basin modelling workflow, the temperature measurements for the 46 analysed 1-D PetroMod models have been converted to heat flow at the well position (Fig. 11). The heat flow in the DCG is in the range ~45 to ~70 mW/m^2, with an increasing trend of heat flow values from low values in the Feda and Gertrud Grabens in the north to high values in the Salt Dome Province in the south, as also reflected in the temperature data itself (Fig. 10B). According to the review of temperatures and heat flow in the North Sea presented by Kubala *et al.* (2003), this distribution is as expected with lowest heat flow in basin centres

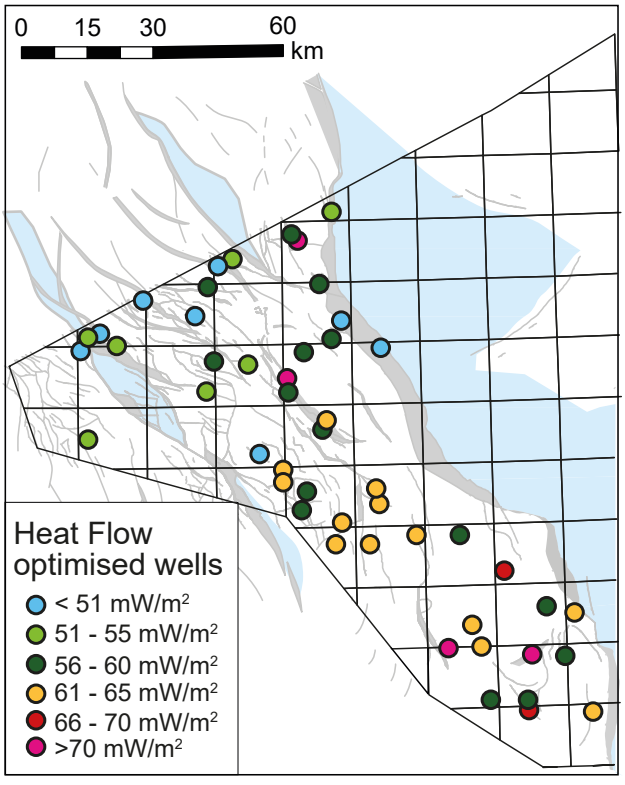

Fig. 11. Heat flow at the well position calculated from 1-D basin models in the Danish Central Graben. Note the general increase in the average values from north to south.

and highest on basin highs associated with conductive rock types. Additional heat is also expected to be associated with fluid migration, which within the DCG supposedly occurs from the high-pressured areas in the north and to low-pressured areas in the south (Japsen 1998; Vejbæk *et al.* 2005).

Maturity modelling

1-D basin modelling

The thermal burial history of 46 well locations was calibrated against the measured VR data and present-day temperatures by adjusting the heat flow history to reach an acceptable match. In our evaluation we used three kinetic models; the Easy% R_o by Sweeney & Burnham (1990), the Easy% R_oDL by Burnham *et al.* (2017) and the Basin% R_o by Nielsen *et al.* (2015) to illustrate the possible ranges in modelled VR.

The most widely used kinetic model is the Easy% R_o. This model, however, has been shown to generally result in calculated higher VR values compared to other models (Nielsen *et al.* 2015). Therefore, a more shallow depth to the start of the oil window (0.6% R_o) was modelled using Easy% R_o. This is illustrated for four selected wells where the oil window (0.6% R_o) is in the range 2.9–3.9 km using Easy% R_o 3.6–4.5

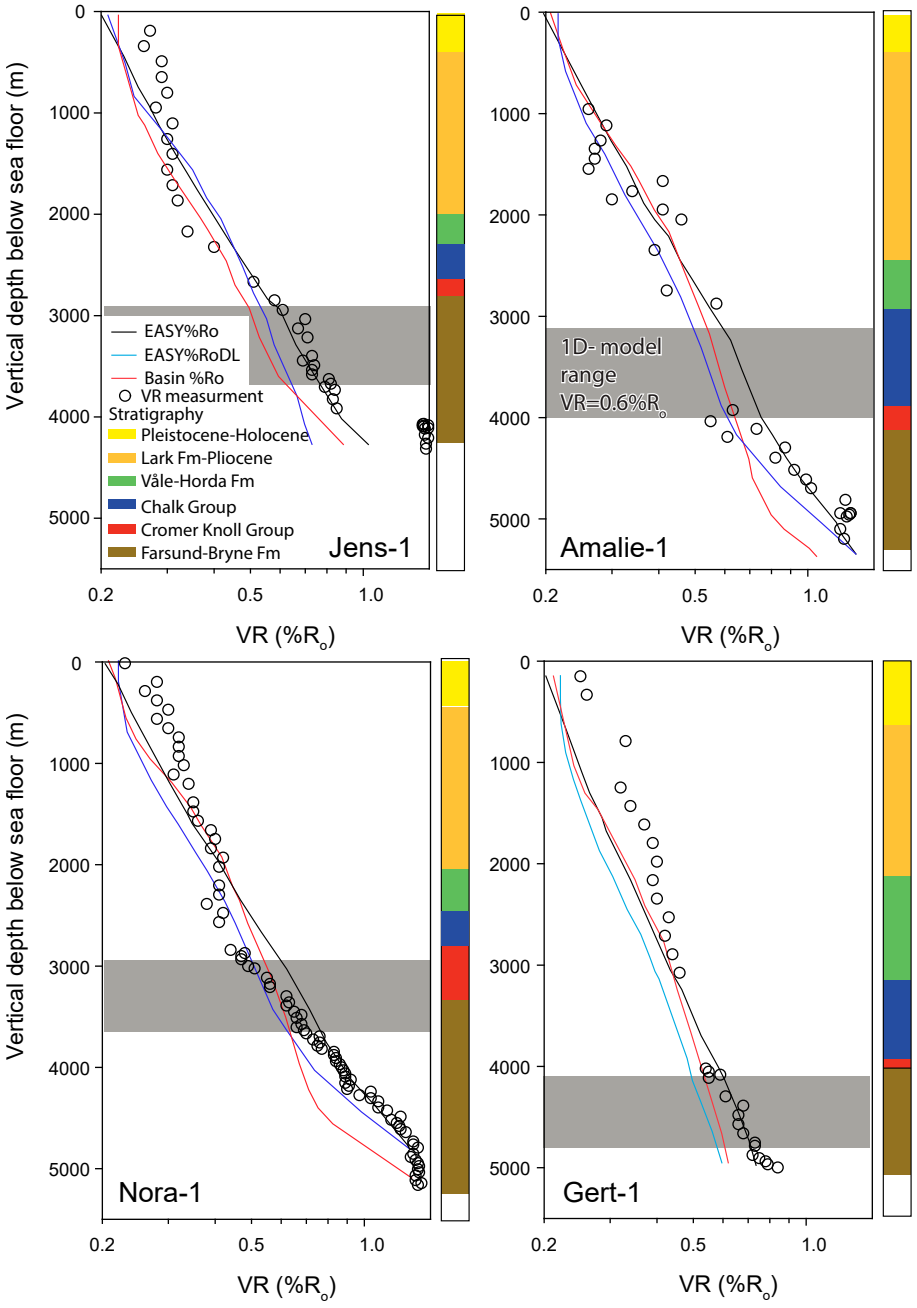

Fig. 12. 1-D basin models of four wells showing modelled VR based on the kinetic models: Easy% R_o (Sweeney & Burnham 1990), Easy% R_oDL (Burnham *et al.* 2017) and Basin% R_o (Nielsen *et al.* 2015). The grey intervals represent minimum and maximum model depths of VR of 0.6% R_o. For stratigraphic units, see Fig. 2.

km using Basin% R_o and 3.3–4.8 km using Easy% Ro DL (Fig. 12). For each well the model differences in the start of the oil window are in the range *c.*700–900 m, with the largest difference for the Amalie-1 (900 m) well and the lowest difference for the Gert-1 and Nora-1 wells (*c.* 700, Fig. 12).

In all 1-D basin models it was difficult to obtain a reasonable match between the modelled VR and the measured VR in the Post Chalk Group (Fig. 12); this is possibly caused by high contents of reworked organic matter, as observed during biostratigraphic studies (Karen Dybkjær, personal communication 2019), which generally tends to result in too high VR. The main emphasis was therefore to obtain a proper calibration match in the Mesozoic sequence using a constant heat flow model through time, as sensitivity studies showed that constant and variable heat flow models provided equally good matches.

Figure 13 shows VR maturity histories obtained using the Easy% R_o kinetic model in the Hejre-1 (Gertrud Graben), the Amalie-1 (Søgne Basin), the Iris-1 and the Svane-1 wells (both Tail End Graben). For these wells, the VR maturity of the uppermost source rock interval (the Ryaz-1 sequence) entered the oil window in the late Palaeogene and reached the main oil window within the last *c.* 5–10 Ma (Fig. 13).

Maturity maps for the Jurassic source rocks

The VR maturities obtained for the 46 1-D models have been compiled into three maturity maps showing the present-day lateral maturity variation for the upper and lower Farsund Formation and for the Middle Jurassic source rocks (Fig. 14). The maps show that the present day maturity for the upper Farsund Formation (the Volg-3–Ryaz-1 sequences) ranges from immature in the southern part of the Salt Dome Province to late oil-mature in and near the Tail End Graben and in the Søgne Basin (Fig. 14A), which is in good agreement with previous maps (Damtoft *et al.* 1987; Thomsen *et al.* 1990).

The underlying part of the Farsund Formation (the Kimm-3–Volg-3 sequences) are immature in local areas but are post-mature with respect to oil generation in the Tail End Graben and the Rosa Basin within the Salt Dome Province (Fig. 14B). The Middle Jurassic Bryne, Lulu and Middle Graben Formations are gas-prone in most of the DCG area (Fig. 14C). No maturity maps are presented for the Lower Jurassic

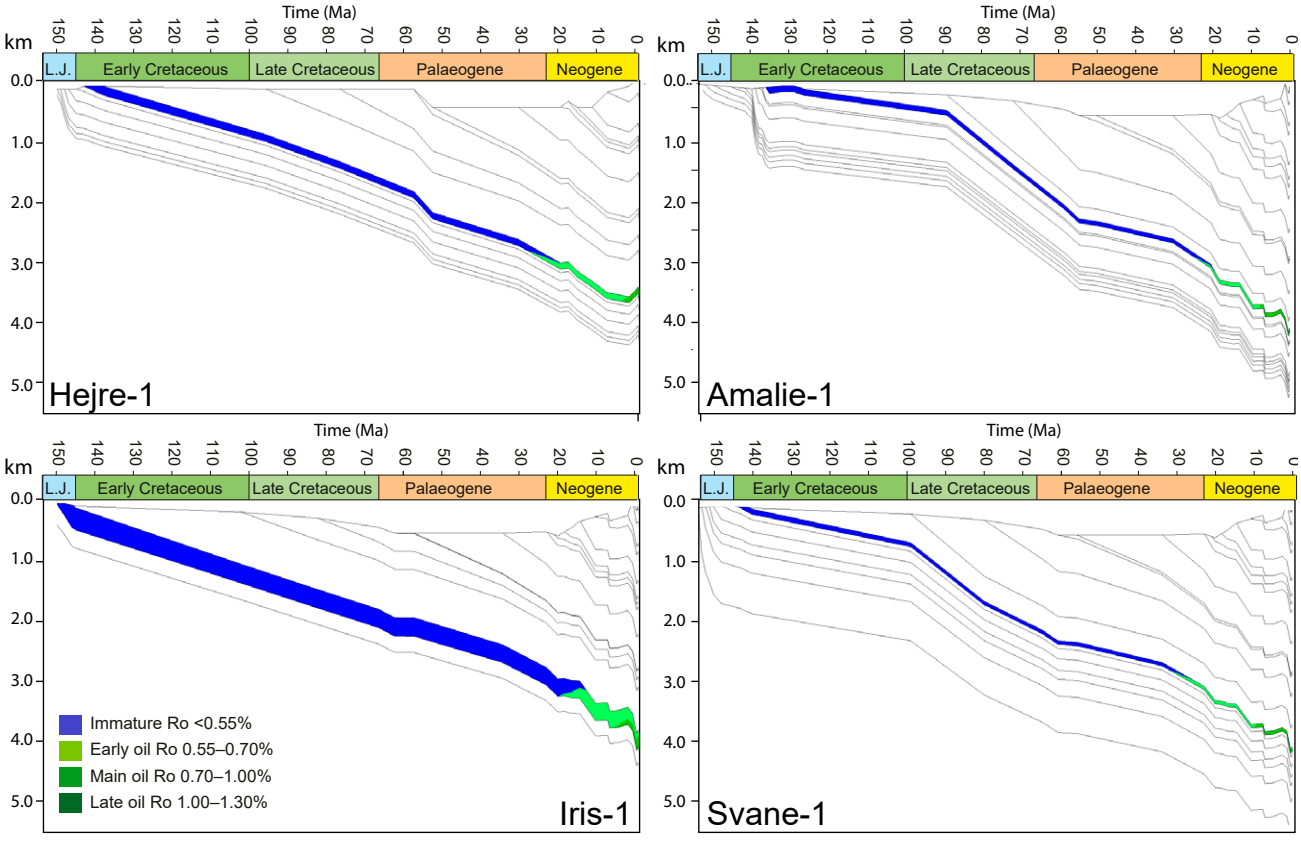

Fig.13. Examples of 1-D burial history at four well locations, showing the VR maturation of the uppermost source rock interval (Ryaz-1 sequence) through time using the Easy% R_o kinetic model. The selected 1-D models show that Ryaz-1 entered the oil window (here assumed at 0.55% R_o) in the late Palaeogene and reached the main oil window within the last *c.* 5–10 Ma.

Fjerritslev Formation and we can only infer that the formation will be more mature than what is mapped for the Middle Jurassic source rocks.

Modelling of VR based on the stratigraphic depths

The 1-D PetroMod modelling of the VR depends on kinetic considerations among many things (see the Basin modelling section); however, VR modelling can also be made solely as a data-driven exercise. For this type of modelling we use the stratigraphic depths as input parameters: the depth below the sea floor, the depth with reference to the top and base of the Chalk Group and the depth with reference to the BCU, i.e. the main stratigraphic levels. For modelling, we applied the PLS regression method as described in the Statistical and regression analysis section.

In the PLS VR-model presented in Fig. 15, a one-component model (Fig. 15B) based on the depth variables predicts the VR with satisfactory validation results as seen in the prediction versus reference plot in Fig. 15C (slope 0.88; $r^2 = 0.88$), suggesting that the PLS VR-model leads to better VR estimates than com-

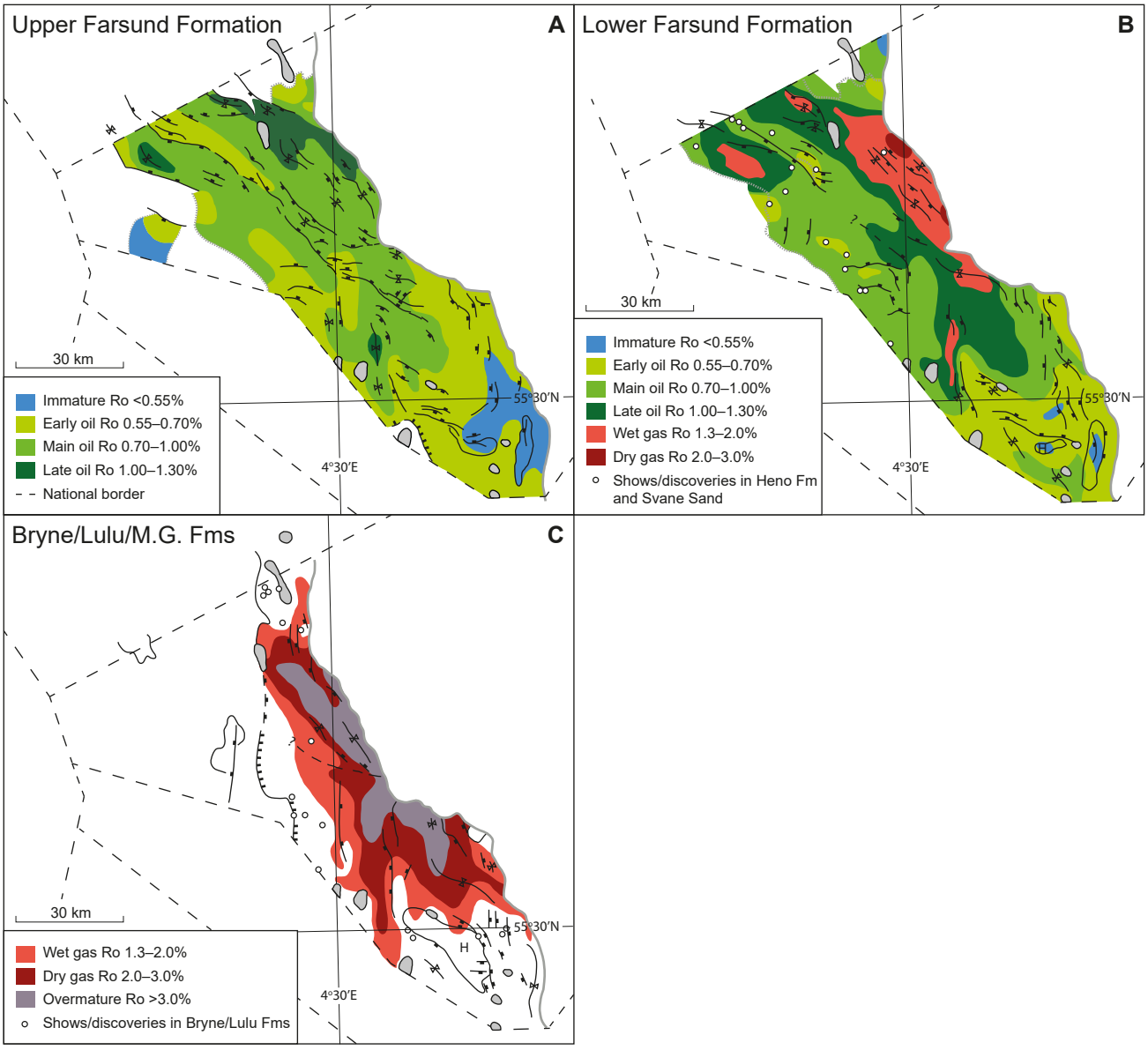

Fig. 14. 1-D modelled maturity based on 46 wells using Easy% R_o to interpolate the maturity. **A:** The upper part of the Farsund Formation (Volg-3–Ryaz-1 sequences); **B:** The lower part of the Farsund Formation (Kimm-3–Volg-2 sequences); **C:** the Lower and Middle Jurassic (from Lower Jurassic to near the top Bryne, Lulu and Middle Graben Formations). Map A is modified from Ponsaing *et al.* (2020b).

monly achieved from any conventional depth plots such as those presented in Fig. 9. In the PLS VR-model, the depth below the sea floor is strongly positively correlated with the VR, as expected, and the depths with reference to the stratigraphic levels are negatively correlated with the VR (Fig. 15A).

The PLS VR-model can be expressed in a manner similar to the regional VR-model (equation 1) as:

$$VR\ (\%\ R_o) = 10^{\ (0.000126 \cdot depth - b)} \quad (4)$$

where depth is measured vertically below sea floor in metres. The constant b is calculated as:

$$b = 0.339 + 3.24 \cdot 10^{-5} \cdot Chalk_{top} + 3.11 \cdot 10^{-5} \cdot Chalk_{base} + 3.15 \cdot 10^{-5} \cdot BCU \quad (5)$$

where $Chalk_{top}$ is the depth in metres below the sea floor of the top of the Chalk Group, $Chalk_{base}$ is the depth in metres below the sea floor of the base Chalk Group and BCU is the depth in metres below the sea floor of the BCU. The constants are derived from the PLS model.

The depth (in metres below the sea floor) to a specific VR value can be found by a simple reorganisation of equation 4:

$$Depth\ (m) = (logVR + b)\ /\ 0.000126 \quad (6)$$

The PLS VR-model predictions for the analysed wells versus depth are shown in Fig. 16A. In the model, wells from the Salt Dome Province generally plot with higher VR than wells from other areas in the DCG. Wells with the lowest VR for a given depth are from the Feda and Gertrud Grabens. This feature is also seen in the original VR data (Fig. 9) and reflects the difference in geological development, notably the Chalk Group thickness. The residual from the PLS VR-model calculated as the difference between measured and modelled VR is generally less than ± 0.1% R_o (Fig. 16B). The PLS VR-model appears to significantly underestimate the VR for Middle Jurassic samples in the Lulu area and for samples in the Lola, Bryne and Middle Graben Formations in the Nora-1, Svane-1, Amalie-1 and Jens-1 wells (Fig. 16B). This reflects that the PLS VR-model is not fine-tuned to specific local conditions. The Lulu area appears to be warmer than generally anticipated and therefore has a different VR-gradient (Petersen *et al*. 2011). The underestimation of the VR in the Lola, Bryne and Middle Graben Formations may reflect differences in facies types or preservation of the organic matter that the model does not account for.

To further illustrate the performance of the PLS VR-model (equation 4 and 5) versus the regional VR-model (equation 1), four wells (Jens-1, Amalie-1, Nora-1, and Gert-1) are shown in Fig. 17. In the diagrams, the measured VRs indicate that the top of the oil window (0.6% R_o, black arrows) is in the range 2.9–4.2 km, with the Jens-1 well (Fig. 17A, Salt Dome Province) and the Gert-1 well (Fig. 17D, Feda and Gertrud Grabens) as the shallowest and deepest examples, respectively.

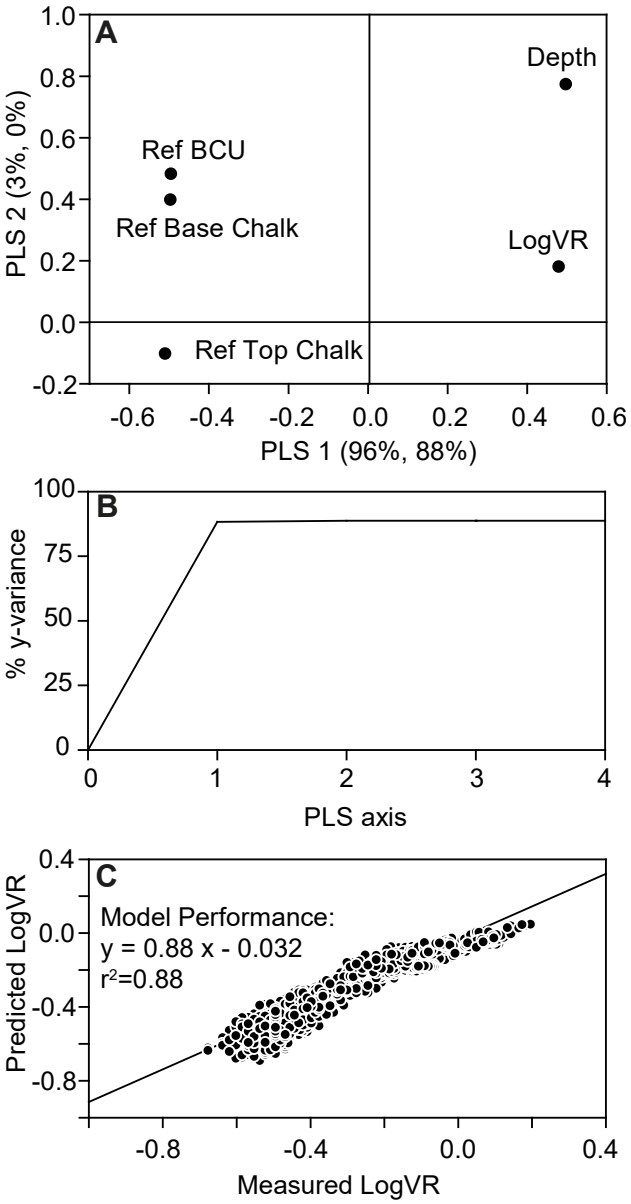

Fig. 15. Partial least squares (PLS) regression model for the logarithm of VR (logVR) and the depth, calculated with respect to different reference surfaces: depth below sea floor (depth), depth with reference to top Chalk Group (Ref Top Chalk), depth with reference to base Chalk Group (Ref Base Chalk) and depth with reference to the Base Cretaceous Unconformity (Ref BCU). **A:** PLS loading-weights plot; **B:** Modelled y-variance; **C:** Predicted logVR versus measured logVR. Outliers were deleted from the original data set in the final PLS VR-model.

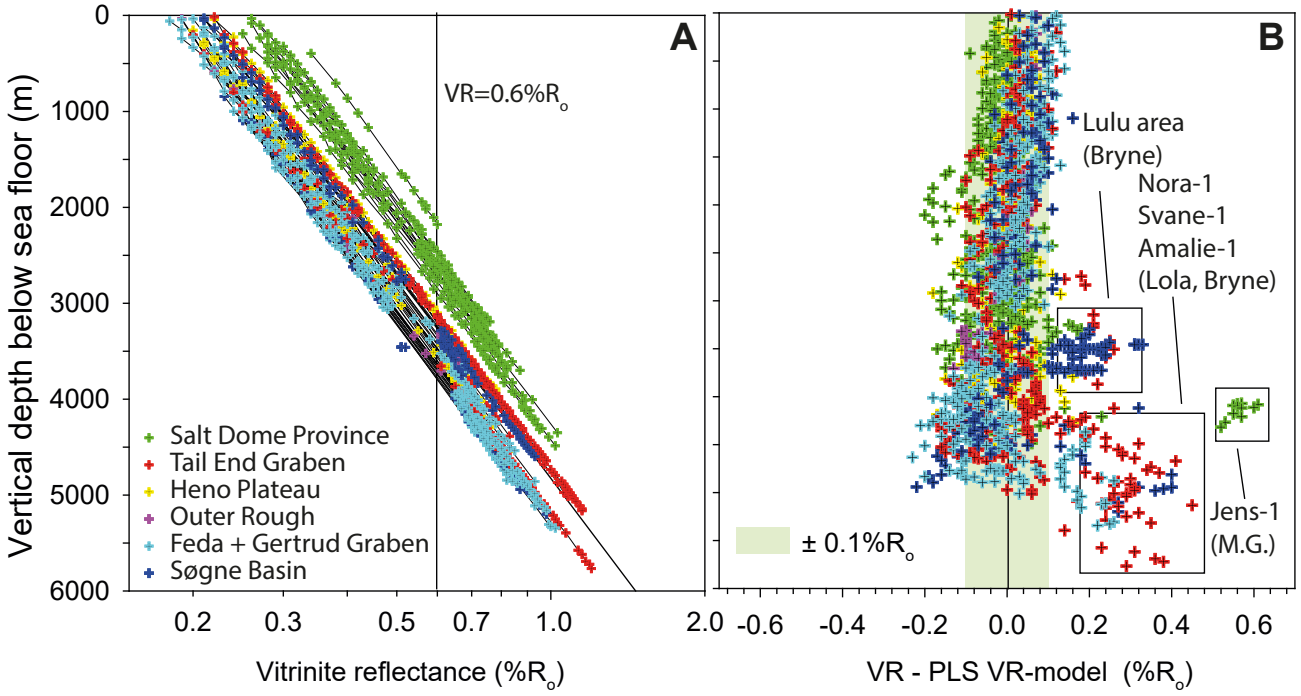

Fig. 16. A: PLS VR-model versus depth below present sea floor; **B:** Residual VR analysis, calculated as Residual VR = Measured VR – PLS VR-model.

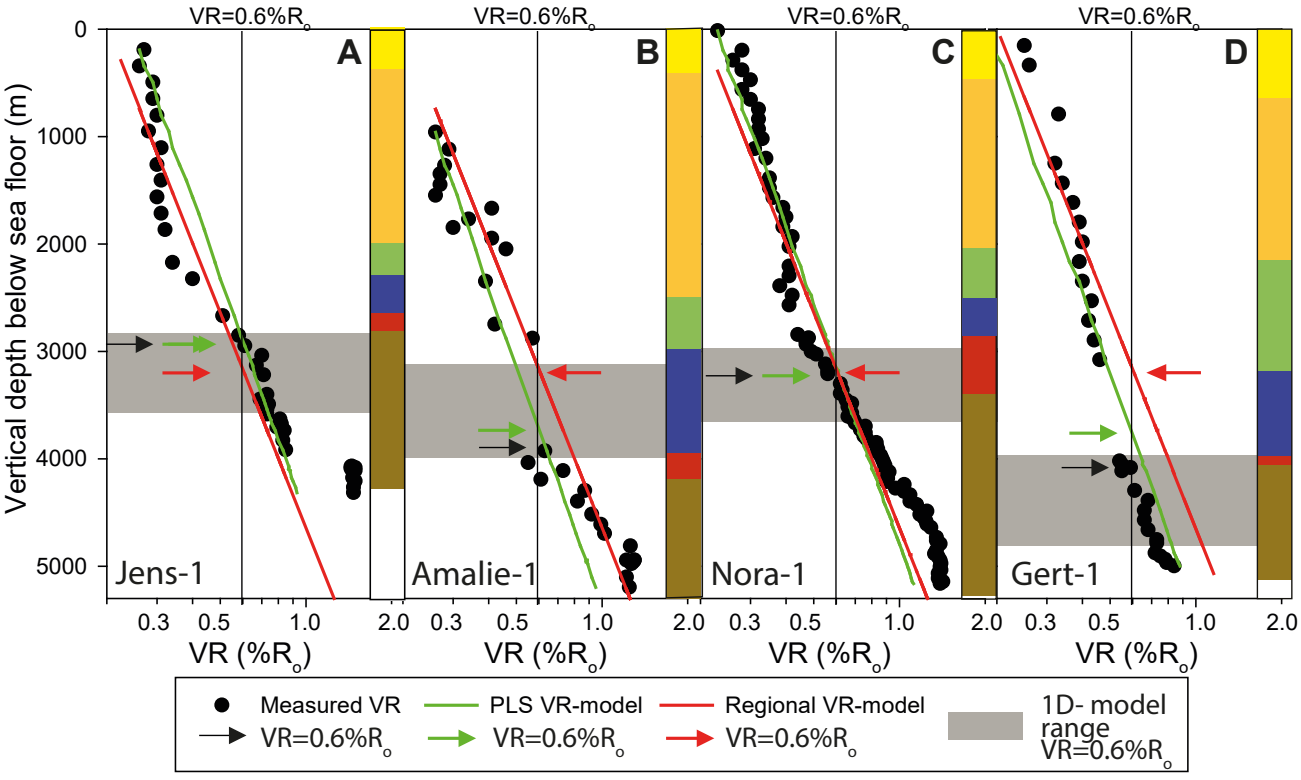

Fig. 17. Vitrinite reflectance (VR) versus depth below sea floor for four wells showing measured VR, the PLS VR-model (equation 4 and 5) and the regional VR-model (equation 1). The grey intervals represent minimum and maximum model depths of VR of 0.6% R_o. For stratigraphic units, see Fig. 2.

Table 3. Stratigraphic depths, depth below seafloor (TVDSF) of VR=0.6% Ro, and the b constant

Well	Area	Top Chalk Group	Base Chalk Group	Top BCU	Depth to 0.6% VR*	b**
		m, TVDSF	m, TVDSF	m, TVDSF	m, TVDSF	
BERTEL-1	Feda/Gertrud Graben	3046	4165	4221	3809	0.701
DIAMANT-1	Feda/Gertrud Graben	2950	3594	3599	3487	0.660
GERT-1	Feda/Gertrud Graben	3037	3820	3905	3642	0.680
GERT-2	Feda/Gertrud Graben	3035	3825	3899	3641	0.680
GERT-4	Feda/Gertrud Graben	3032	3804	3860	3625	0.678
HEJRE-1	Feda/Gertrud Graben	2996	3594	4194	3647	0.681
JEPPE-1	Feda/Gertrud Graben	3060	4074	4279	3804	0.700
KARL-1	Feda/Gertrud Graben	2956	4084	4164	3751	0.694
LONE-1	Feda/Gertrud Graben	2879	3185	3414	3321	0.639
MONA-1	Feda/Gertrud Graben	2927	3343	3893	3492	0.661
OPHELIA-1	Feda/Gertrud Graben	3065	4023	4339	3808	0.701
Q-1X	Feda/Gertrud Graben	2972	3865	3907	3636	0.679
RITA-1X	Feda/Gertrud Graben	2967	3336	3665	3443	0.655
STEN-1	Feda/Gertrud Graben	2951	3161	3926	3462	0.657
2/12-1	Feda/Gertrud Graben	3014	3824	3895	3634	0.679
2/11-7	Feda/Gertrud Graben	2980	3525	3678	3497	0.662
´2/5-9	Feda/Gertrud Graben	3168	3992	4046	3753	0.694
EDNA-1	Heno Plateau	2643	2932	2991	3091	0.611
ELLY-2	Heno Plateau	2782	3422	3425	3357	0.644
FALK-1	Heno Plateau	2821	3523	3523	3417	0.652
RAVN-1	Heno Plateau	2969	3712	3712	3549	0.668
RAVN-2	Heno Plateau	2976	3651	3651	3521	0.665
SKARV-1	Heno Plateau	2655	3293	3318	3266	0.633
W-1X	Heno Plateau	3001	3673	3673	3538	0.667
KIM-1	Outer Rough	3048	3803	4003	3665	0.683
TORDENSKJOLD-1	Outer Rough	2778	3240	3303	3280	0.634
ALMA-1X	Salt Dome Province	1979	2425	2487	2668	0.557
ANNE-3	Salt Dome Province	1786	2276	2357	2549	0.542
BO-1X	Salt Dome Province	1981	2199	2467	2608	0.550
E-1X	Salt Dome Province	1977	2413	2890	2766	0.570
FASAN-1	Salt Dome Province	2019	2370	2660	2708	0.562
G-1X	Salt Dome Province	1927	2134	2311	2539	0.541
JENS-1	Salt Dome Province	2305	2580	2814	2873	0.583
JOHN-FLANKE-1	Salt Dome Province	1480	1618	1618	2122	0.489
M-8X	Salt Dome Province	1761	2119	2201	2465	0.532
NORTH-JENS-1	Salt Dome Province	2019	2141	2352	2575	0.546
O-1X	Salt Dome Province	1787	2234	2311	2527	0.540
OLGA-1X	Salt Dome Province	1868	2436	2569	2663	0.557
S.E. IGOR-1	Salt Dome Province	1944	2013	2051	2448	0.530
SKJOLD FLANK-1	Salt Dome Province	2050	2694	2779	2829	0.578
U-1X	Salt Dome Province	2152	2400	2424	2691	0.560
AMALIE-1	Søgne Basin	2946	3903	4096	3686	0.685
CLEO-1	Søgne Basin	2732	3219	3219	3243	0.630
Gita-1	Søgne Basin	3158	3985	4026	3744	0.693
LULITA-1X	Søgne Basin	2822	3261	3261	3287	0.635
LULU-1	Søgne Basin	2656	3148	3148	3187	0.623
WEST LULU-1	Søgne Basin	2771	3398	3398	3342	0.642
WEST LULU-2	Søgne Basin	2813	3515	3515	3410	0.651
WEST LULU-3	Søgne Basin	2774	3423	3423	3355	0.644
XANA-1X	Søgne Basin	3009	4108	4232	3788	0.698
BARON-2	Tail End Graben	2725	2852	3321	3175	0.621
ELIN-1	Tail End Graben	2636	2855	3453	3186	0.623
GULNARE-1	Tail End Graben	2883	3839	4219	3685	0.685
I-1X	Tail End Graben	2670	2757	3266	3124	0.615
IRIS-1	Tail End Graben	2806	3117	3832	3390	0.648
NORA-1	Tail End Graben	2511	2813	3389	3128	0.615
STORK-1	Tail End Graben	2838	3862	3925	3606	0.675
SVANE-1	Tail End Graben	2859	3700	4003	3590	0.673

*Calculated from equation 4. **Calculated from equation 3. TVDSF: Total vertical depth below sea floor.

For all wells, the regional VR-model (equation 1, red arrows) predicts the top of the oil window to be at 3.2 km, whereas in the PLS VR-model (equation 4 and 5, green arrows) it is in the range 2.9–3.8 km (Fig. 17). Based on the PLS VR-model, a thin Chalk Group as in the Jens-1 well leads to a more shallow position of the oil window, whereas a thick Chalk Group as encountered in the Amalie-1 and Gert-1 wells (Fig. 17C, D) will lead to a deeper position of the oil window as compared to the regional VR-model. The thickness of the Cromer Knoll Group also affects the oil window position by shifting it to deeper levels as seen in the Nora-1 well (Fig. 17C).

Compared to the 1-D basin models for the VR development (Fig. 12), the PLS VR-model for the start of the oil window is within their range for the Jens-1, Amalie-1 and Nora-1 wells but is several hundred metres too shallow with respect to predicting the onset of the oil window in the Gert-1 well (Fig. 17). This demonstrates that the PLS VR-model should only be used as a first guide to the VR development. However, once established, the model can also be applied to regional depth structure maps as presented in Fig. 5 that will allow for between-wells maturity prediction.

Based on the PLS VR-model, the depth to the oil window (0.6% R_o) has been mapped in the investigated wells (Fig. 18; Table 3). In the Salt Dome Province, the start of the oil window is modelled to occur between 2.2 and 3.2 km, whereas deeply positioned oil windows are modelled in the northern part of the DCG, especially in the Feda and Gertrud Grabens and in the northern Tail End Graben where depths down to *c.* 3.8 km are seen for Bertel-1, Jeppe-1, and Ophelia-1 (Fig. 18, Table 3). The modelling agrees with Petersen *et al.* (2012) who also demonstrated a considerable depth to the top of the oil window in this part of the DCG.

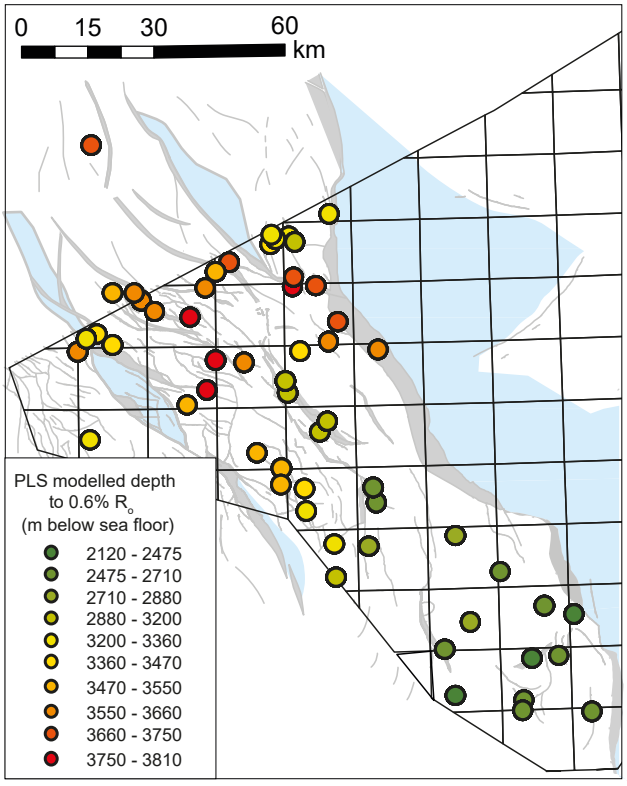

Fig. 18. Modelled depth below sea floor of the top oil window (VR = 0.6% R_o) based on the PLS VR-model. For details see Table 3. See Fig. 1 for map legend.

Discussion

Representativeness of the source rock database

The data used for this study represent nearly four decades of analytical work. There has been no fundamental change in analytical concepts, and although instruments have changed over time, they have all been calibrated in the same way. Experience shows that the variability in data output between instruments generally is within the analytical precision. Hence, data are generally comparable over time. More important and often overlooked are variations introduced by the drilling operations and subsequent sampling for analysis, i.e. prior to analysis in the laboratory (Minkkinen 1987). Our data derive from analysis of both cuttings and core samples. For obtaining representative average compositions for a formation, using cutting samples are not problematic if the sampling is unbiased, i.e. if all lithologies have equal chances of being sampled. Biases may occur if the lithologies have very different behaviours towards the drill bit. In a mixed shale–sand sequence, less cemented sandy beds may thus be under-represented in the analysed cuttings fraction. Similarly, in shales with cemented limestone beds the latter may be over-represented in the cuttings fraction. In addition, cavings may obscure the lithological information of the cutting sample. These effects are here sought minimized by selecting a specific size fraction for analysis, namely the 1–4 mm fraction. Hence, both large-size cavings and very tiny recycled fractions from the drilling mud system are removed.

The second major cause for uncertainty stems from under- or over-sampling of the lithological variation. The minimum sampling frequency aimed at here is 1 sample every 10 m. For the whole sample database, the average is 1 sample every 8 m, as the 5537 samples were picked from a cumulated 44.5 km long interval. However, this estimate does not include the total interval depth and the real sampling frequency is less.

Moreover, the sample count includes core sections where the sampling frequence is much higher than in un-cored sections, resulting in a relative over-representation. In most cases, the sampling has excluded in particular sandy intervals, thus directing the sampling towards the shaly part of the formations. However, the definition of the unsampled lithology is not necessarily the same for a sample database such as the one examined, which reflects decades of sampling. Likewise, we note that in a few cases the reported samples were filtered to exclude samples with less than 0.5 wt% TOC.

Currently, the effects of the above-mentioned errors and biases on our calculated formation averages cannot be quantified. Hence, our interpretations come with this uncertainty. However, comparing core data with data obtained from cuttings is one way to probe the errors associated with some of the drill processes. Also, the resulting organic-richness interpretation can be compared to similar interpretations obtained from carefully calibrated well logs following models such as the delta log R technique of Passey *et al.* (1990), as a judgment based only on the natural gamma log alone is not advisable (Petersen *et al.* 2017). This method will also be highly valuable in cases where an oil-based mud system has made source rock analysis impossible, as seen in the Jude-1 well from the DCG (Petersen *et al.* 2017).

Source rock quality

As advised by Cornford *et al.* (1998), we have used a log-normal distribution model to calculate the population statistics, as the distributions are right-end skewed and thus not compatible with a normal distribution. Using the arithmetic mean ± standard deviation will result in an underestimation of the source rock properties because the standard deviation ignores the extreme distributions that are captured by a log-normal distribution. Hence, the statistical properties presented in Table 2 of the present-day properties allow a much better representation of the data for further analysis.

Compared to the estimation of source-rock richness and quality of the Farsund Formation published by Ponsaing *et al.* (2018), it should be noted that Ponsaing *et al.* (2018) only used a limited data set (13 wells) and that the samples were filtered to include only samples with HI > 200 mg HC/g TOC in order to focus the analysis on oil-prone samples and to limit the effects of maturity on the averages (Ponsaing *et al.* 2018). Compared to the tabulation presented in Table 2 this means that their TOC and HI estimates are within the P50–P10 range reported here.

Lower Jurassic source rocks

The amount of data on the Fjerritslev Formation has increased little since the reviews by Damtoft *et al.* (1987, 1992). The Toarcian part of the Fjerritslev Formation is considered absent in DCG (Fig. 3; Damtoft *et al.* 1987, 1992). Elsewhere in north-western Europe this stratigraphic level includes highly oil-prone intervals assigned to the Posidonia Shale Formation, which is a stratigraphic equivalent to the Fjerritslev Formation. The Posidonia Shale Formation is the most important source rock for oil onshore Germany and the source rock of the Mittelplate field in the German North Sea, which is the largest German oil field situated in the Wadden Sea (Müller *et al.* 2020). In the southern North Sea area, the Posidonia Shale Formation is only preserved in Mesozoic rift basins and in deeper subsided basin parts in the Central Graben (Lokhorst 1997). Remnants of the Posidonia Shale Formation are also assumed to be present in the German Central Graben but are not confirmed by wells (Arfai & Lutz 2018). In the DCG the Fjerritslev Formation has oil/gas generative potential (Table 2) and may provide an additional source. The main uncertainties with regard to this source are the lack of special oil chemistry that may serve to identify a possible contribution, and the very patchy distribution of the formation in the DCG (Michelsen *et al.* 2003).

Middle Jurassic source rocks

One of the major changes in source rock understanding in the DCG since the review by Damtoft *et al.* (1987) is the recognition of the Middle Jurassic Petroleum System (see review by Petersen & Hertle 2018). The coaly source rock is primarily gas-prone but has an average restored HI of about 280 mg HC/g TOC which illustrates the ability to generate liquid hydrocarbons. Paralic parts of the coal beds have a higher generative potential than the landward parts, however the most significant impact on source rock quality is the presence of sapropelic lacustrine facies (Petersen & Hertle 2018). The source rock type is proven as an efficient petroleum system in the DCG in the Harald East and Harald West gas/condensate fields and the Lulita oil field. Outside the DCG it is proven in the Norwegian Trym gas/condensate field and in the UK sector in the large Culzean Field (Petersen *et al.* 2019).

Upper Jurassic–lowermost Cretaceous source rocks

Variation of kerogen type and richness for the DCG was mapped by Damtoft *et al.* (1987), based on just a few wells combined with a conceptual approach in which the depositional depth had a strong control on the maceral types. Hence it was assumed that the most oil-prone kerogen and TOC rich sources occurred in the deepest parts of the basin, where alginites were

expected predominantly to accumulate. In contrast to this, more lean shales dominated by vitrinite and waxy land plant cuticles were expected to accumulate more shorewards (Damtoft *et al.* 1987).

Damtoft *et al.*'s (1987) model predictions are quite similar to the geographical variation in source rock quality and richness documented here (Table 2). However, their stratigraphic constraints were poor, and we apply a much more precise sequence stratigraphic frame that allows us to analyse the source rock variation with an unprecedented high level of detail. We can thus unambiguously show that the south-to-north increase in TOC content exists not only for the topmost Bo Member (i.e. the Volg-4 to Ryaz-1 sequence, Ineson *et al.* 2003) but also for all other analysed sequences in the Farsund Formation (Fig. 8). This suggests that long-lasting controls on the accumulation exerted a first order control on the quality. This control was likely related to the depositional depth of the different basin areas which influences the sea-floor oxygen conditions and depositional energy by preserving the organic matter from decomposition and allows more fine-grained particles to settle. High HI thus reflects dominance of well-preserved marine organic matter, whereas low HI reflects mixed organic matter types and least well-preserved marine types. Such regional variation in source rock quality and richness is not surprising, given that a similar considerable variation has been mapped in a succession that is time-equivalent to the Farsund Formation, namely the Draupne Formation in the South Viking Graben (Justwan *et al.* 2005).

We have not reconstructed the source rock quality to its original pre-productive state, and the regional changes in generative potential is somewhat overprinted by maturity effects (Ponsaing *et al.* 2020a,b). We thus clearly observe that all analysed mature sequences have similar or slightly lower HI values compared to the immature Salt Dome Province (Fig. 8). The present-day mixed oil/gas generative potential of most mature sequences was thus likely much more oil-prone in the northern part of the DCG, as our data in Table 2 suggest. Studies of the kerogen types in the DCG have mostly focused on the stratigraphic control on the oil richness and little regional comparison has been made (Petersen *et al.* 2010, 2017; Ponsaing *et al.* 2018, 2020a,b). According to these studies, the stratigraphic variation in oil richness, as expressed by the HI, is mimicked by changes in the organic macerals type, such as amorphous organic matter. Overall, the Kimmeridgian, i.e. the Lola Formation to lower Farsund Formation, witnessed a transition from more terrestrial-influenced to more open marine conditions which followed the transgression of the DCG (Andsbjerg & Dybkjær 2003; Johannessen *et al.* 2010). The regional variation suggests that tectonic control also played a major role in determining the source rock quality and we thus consider structural topography and the location of sediment input centres to be the ultimate controlling factors, as also put forward by Ineson *et al.* (2003) and Ponsaing *et al.* (2018).

Factors influencing the depth of the oil window

The depth of the oil window, as defined by a VR of 0.6% R_o, is in the range 2200–4500 m in the DCG (Fig. 9A). This depth variation can be modelled by using a simple depth model, the VR PLS-model, that includes the thickness of the Palaeogene to Cretaceous Chalk and Cromer Knoll Groups in the VR prediction (Fig. 15). According to this model, a thick Chalk Group offsets the oil window to deeper levels as expected from a regional point of view. An explanation that links a deeply positioned oil window to areas with a thick Chalk Group (see Fig. 5D) was put forward by Petersen *et al.* (2012), based on wells in the northern part of the DCG. These authors attributed the effect to the thermal properties of the highly thermally conductive chalk, in contrast to the underlying lesser thermally conductive clays. In addition to this, they also invoked a highly overpressured system at the base of the Chalk Group to cause an additional downward displacement of the oil zone, following Carr (1999). Nielsen *et al.* (2015) modelled some of the wells analysed by Petersen *et al.* (2012) and did not find any overpressure effects on the position of the oil window. Instead, they attributed the deep position of the oil window solely to thermal conductivity differences between chalk and shale.

Our analysis of the temperature and pressure data (Fig. 10) does not indicate that specific parts of the deeper DCG is more pressurised, as all wells at depth follow the same overall trend. Instead, we find that the temperature and its translation into heat flow (Figs 10B, 11) within the DCG varies in a manner that mirrors the depth differences to the top of the oil window. We therefore also consider that temperature differences are the main cause of the depth differences of the top of oil window (Fig. 18).

In basin modelling, the onset of the oil window can be assessed after the model has been calibrated against particularly heat flow, thermal conductivities and kinetic models. The most widely used kinetic model is the Easy% R_o kinetic model by Sweeney & Burnham (1990). However, due to uncertainties regarding the kinetic model for the calculation of VR based on a given temperature history, alternative kinetic models have been developed over the last years (Nielsen *et al.* 2015). These models address various issues such as compu-

tational time, effects of pressure and importance of vitrinite suppression due to differences in deposition conditions and maceral interactions. During the last years, it has been argued that the Easy% R_o kinetic model has some weaknesses and that the calculated values are higher than the measured values. Thus, it is currently uncertain whether a universal algorithm for VR prediction exists, because maturation of vitrinite and oil-prone kerogen may require local/basin-wide corrections for the individual kerogen types, as different calibrations of the kinetic model will be required for vitrinite in coals and oil-prone organic matter (Schenk *et al.* 2017).

The PLS VR-model applied here in addition to the kinetic-based VR-models offers an independent and data-driven approach to VR-modelling. This type of modelling has shown to provide results comparable to the kinetic-based models for predictions of the present day maturity profiles (Fig. 17), but it does not provide any understanding of the timing or dynamics in the maturity development, as the kinetic models do (Fig. 13). Instead, data-driven models such as the PLS VR-model applied here may help to provide constraints on the boundary conditions and other needed input parameters to more sophisticated models that properly constrained will outperform simpler models.

Source rocks quality and oil types

Oil sourced from Middle and Upper Jurassic source rocks can be clearly distinguished from each other and from Permian sources based on oil chemistry (Petersen *et al.* 2016; Schovsbo *et al.* 2018). Among the marine Jurassic oil types (type 1 of Schovsbo *et al.* 2018), four subtypes have been recognised. Of these, two subtypes have contributed significantly to the accumulated oils, namely a 'Tail End type' (1A type) that occurs in all fields bordering the Tail End Graben and in the Siri Canyon, and a 'Salt Dome type' (1D type) that occurs in the southern part of the Salt Dome Province (Fig. 19). Compared to our findings on source rock quality and maturity variation in the DCG, the two main types can be related to both the stratigraphic and the regional variation in source rock quality and maturity. Type 1A is thus characterised by high bisnorhopane biomarker content indicative of strong marine anoxic conditions as typically found in the Bo Member (Ineson *et al.* 2003; Petersen *et al.* 2016; Ponsaing *et al.* 2020a,b). Type 1D has a similar affinity to marine anoxic conditions but has less bisnorhopane. The dominance of type 1A in the Tail End Graben thus reflects both the thick succession with excellent source rock qualities here and the mature nature of

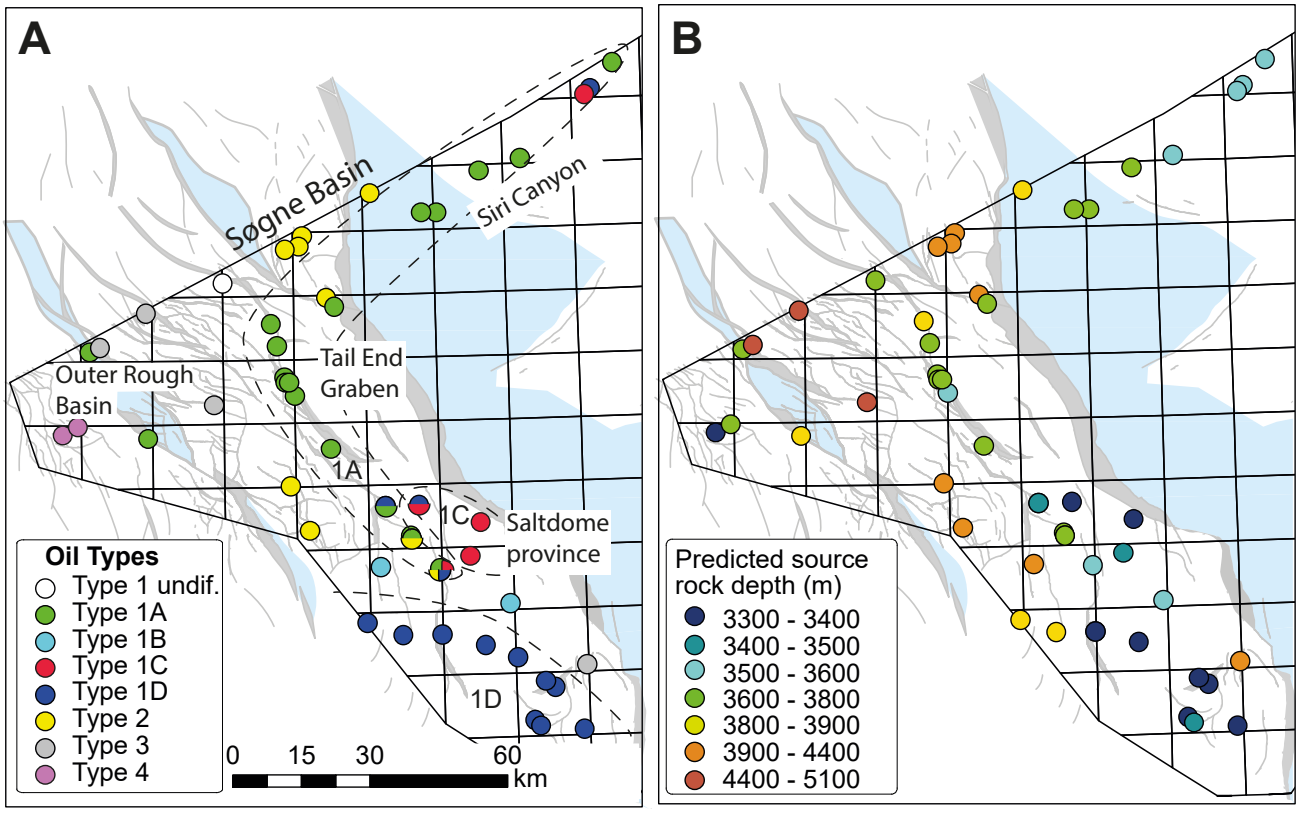

Fig. 19. A: Oil types and **B:** relative oil maturity as depicted by modelled source rock depth. Shallow depths in B indicate less mature oils. Modified from Schovsbo *et al.* (2018). See Fig. 1 for map legend.

the unit. The presence of type 1D oil in the Salt Dome Province is interpreted to reflect other sources than the uppermost Farsund Formation as this is generally immature here and has less good source rock qualities (Ponsaing *et al.* 2020a).

The oil type potentially generated from the Fjerritslev Formation is poorly known in the DCG, as the biomarker compositions are only described from five source rock extracts (Schovsbo *et al.* 2018). Of these, the biomarker composition of two source rock extracts (from the M-8X and Skarv-1 wells) cannot be matched with any reservoired oil, whereas of three source rock extracts one is a pure terrestrial (type 3, U-1X well), one has a marine anoxic signature 'Tail End type' (type 1A, Jens-1 well), and one is an oil type known to occur in the Adda and Boje fields (type 1C, N-22X well). Currently, it is not known if this variability reflects the rock itself or migrated oils from other source rock levels. Based on the source rock screening data, the compositional variation may be a reflection of the bimodal HI distribution, which suggests that the formation has both terrestrial mixed oil/gas-prone and highly oil-prone generative potential (Fig. 7). Unpublished GEUS data suggest that the highly oil-prone Toarcian part of the Posidonia Shale Formation in south-west Germany has a biomarker composition different from those in the DCG (Peter Nytoft, personal communication May 2019). The Toarcian part of the Fjerritslev Formation is also not considered to be present in the DCG (Fig. 2), and further studies will aim at characterising the Lower Jurassic source rock biomarker signature.

Terrestrial-influenced oils (type 2 and 3 of Schovsbo *et al.* 2018) are, among many other features, characterised by much higher pristane/phytane ratios than the fully marine Jurassic types (Petersen *et al.* 2016; Schovsbo *et al.* 2018). Type 2 occurs in the Søgne Basin, including the northern part of the Tail End Graben, and on the eastern Heno Plateau (Fig. 19). These occurrences are within the Middle Jurassic Petroleum System and reflect oil sourced from the Bryne and Lulu Formations, as recently reviewed by Petersen & Hertle (2018). Type 3 has been documented from oil stains in the Alma-2, Bertel-1, Gert-1and Rita-1 wells (Fig. 19), and from source rock extracts it is known to occur in the Middle Jurassic Bat-1 to Upper Jurassic Kimm-3 sequences (Schovsbo *et al.* 2018). These sequences all contain terrestrial-dominated, gas-prone kerogen (Table 2; Ponsaing *et al.* 2018).

High-pressure, high-temperature conditions within the Danish Central Graben

The DCG is an overpressured basin with several known pressure seals including Paleocene shales, intra-chalk seals, Lower Cretaceous shales and intra-Jurassic shales. This leads to rapid fluid pressure build-ups and mean fluid pressures considerably higher than hydrostatic (Japsen 1998; Dennis *et al.* 2005; Vejbæk 2008; Petersen *et al.* 2012), as shown in Fig. 10.

HPHT hydrocarbon exploration in the DCG is by some authors considered to include areas with fluid pressures above 70 MPa and temperatures above 150°C (i.e. Smithson 2016). Following this definition, the required pressure regime based on our observations in Fig. 10A is expected to occur from below 3.8 km depth. Likewise, temperatures above 150°C are expected to be reached at around the same depth in most areas of the DCG except for the Feda/Gertrud Graben, where it is expected to be reached around 4.7 km (Fig. 10B). Using these depths as guideline, the HPHT regime includes the Hejre Field and the Amalie-1, Svane-1 and Xana-1X discoveries (Fig. 2).

Conclusions

The Danish Central Graben is a mature petroleum province with the principal petroleum source rocks being the Upper Jurassic – lowermost Cretaceous marine Farsund Formation shales and with minor contributions from Middle Jurassic coaly units of the Lola, Bryne and Lulu Formations.

Statistical parameters (average, median, low (P90) and high (P10) percentiles) describing the present day distribution of TOC, HI and T_{max} are presented for the Lower Jurassic marine Fjerritslev Formation, the Middle Jurassic Bryne, Lulu, and Middle Graben terrestrial-paralic formations, and the Upper Jurassic-lowermost Cretaceous marine Lola and Farsund Formations in six areas in the DCG. In calculating the parameters a log-normal distribution model has been used, allowing a strongly improved representation of the data for further analysis.

Within the DCG a clear south-to-north increase in TOC level exists not only for the topmost Bo Member of the Farsund Formation but also for all other analysed sequences in the Farsund Formation.

Two maturity maps of the upper and lower part of the Farsund Formation and one representing the Middle Jurassic formations show that the upper Farsund Formation is immature in the southern part of the Salt Dome Province and in the late oil mature in and near the Tail End Graben and the Søgne Basin. The lower part of the Farsund Formation is immature in local areas but post-mature in the Tail End Graben and in the Rosa Basin within the Salt Dome Province. The Lower Jurassic and the Middle Jurassic Bryne,

Lulu and Middle Graben Formations are gas-prone in most of the DCG.

1-D basin modelling shows that the uppermost source rock interval (the Ryaz-1 sequence), illustrated by four representative deep wells in the Gertrud Graben, Søgne Basin and Tail End Graben, entered the oil window in the late Palaeogene, reaching the main oil window within the last *c.* 5–10 Ma.

The depth of the oil window, as defined by a vitrinite reflectance of 0.6% R_o, ranges between 2200 and 4500 m in the DCG. Much of this variation in depth can be modelled by using a simple depth model, the PLS VR-model, that includes the thickness of the Palaeogene to Cretaceous Chalk and Cromer Knoll Groups in the VR prediction. According to this model a thick Chalk Group offsets the oil window to deeper levels. The reason for this can be attributed to the thermal properties of the highly thermally conductive chalk in contrast to the underlying lesser thermally conductive clays. Higher modelled thermal heat flow in the Salt Dome Province likely also contributed to a more shallow position of the oil window in this part of the DCG.

Our findings on source rock quality and maturity variations in the DCG add further to the effective source rock intervals that gave rise to the two main Jurassic oil types in the DCG. The dominance of type 1A in the Tail End Graben thus reflect both the thick succession with excellent source rock qualities and the mature nature of the Bo Member of the Farsund Formation. The presence of the Type 1D oil in the Salt Dome province is interpreted to reflect other Jurassic sources that the uppermost Farsund Formation.

The source rock screening data show that the compositional variation of the Fjerritslev Formation indicates both a gas- and a highly oil-prone generative potential. The source rock extracts from the formation is very limited and variable, and it is unknown if this variability reflects the rock itself or migrated oils from other Jurassic source rock levels.

The DCG is an overpressured basin. High fluid pressures > 70 MPa and high temperatures > 150°C are expected to occur deeper than 3.8 km except for the Feda and Gertrud Grabens where it is expected to be effective from around 4.7 km depth due to general lower temperatures here.

Acknowledgement

This paper is published with permission from the Geological Survey of Denmark and Greenland. We thank Ineos E&P A/S and its partners (Danoil Exploration A/S and Nordsøfonden) in licence 9/95 for financial support of part of this study. Most data originate from databases compiled during the industrial multi-client studies PETSYS and CRETSYS, both led by GEUS. Erik Thomsen is thanked for his contribution to these projects. Ditte Kiel-Dühring and Carsten Guvad are acknowledged for carrying out most of the analytical work presented here. Comments and suggestions from the journal reviewers Henrik Ingermann Petersen and Hamed Sanei and the editor Lotte Melchior Larsen are highly appreciated and significantly improved the quality of the paper. The paper is a contribution to the EU Horizon2020 GeoERA project (GARAH, H2020 grant #731166 led by GEUS).

References

Anderskouv, K. & Surlyk, F. 2011: Upper Cretaceous chalk facies and depositional history recorded in the Mona-1 core, Mona Ridge, Danish North Sea. Geological Survey of Denmark and Greenland Bulletin 25, 60 pp. https://doi.org/10.34194/geusb.v25.4731

Andsbjerg, J. & Dybkjær, K. 2003: Sequence stratigraphy of the Jurassic of the Danish Central Graben. Geological Survey of Denmark and Greenland Bulletin 1, 265–300. https://doi.org/10.34194/geusb.v1.4675

Arfai, J. & Lutz, R. 2018: 3D basin and petroleum system modelling of the NW German North Sea (Entenschnabel). Geological Society, London, Petroleum Geology Conference series 8, 67–86. https://doi.org/10.1144/PGC8.35

Burnham, A.K, Peters, K.E. & Schenk, O. 2017: Evolution of vitrinite reflectance models. Search and Discovery Article #41982, 23 pp.

Carr, A.D. 1999: A vitrinite reflectance kinetic model incorporating overpressure retardation. Marine and petroleum geology 16, 355–377. https://doi.org/10.1016/S0264-8172(98)00075-0

Cornford, C., Gardner, P. & Burgess, C. 1998: Geochemical truths in large data sets. I: Geochemical screening data. Organic geochemistry 29, 519–530. https://doi.org/10.1016/S0146-6380(98)00189-2

Damtoft, K., Andersen, C. & Thomsen, E. 1987: Prospectivity and hydrocarbon plays of the Danish Central Trough. In: Brooks, J. & Glennie, K.W. (eds), Petroleum geology of North-West Europe, 403–417. London, Graham & Trotman.

Damtoft, K., Nielsen, L.H., Johannessen, P.N., Thomsen, E. & Andersen, P.R. 1992: Hydrocarbon plays of the Danish Central Trough. In: Spencer, A.M. (ed.), Generation, Accumulation and Production of Europe's Hydrocarbons II. 35–58. Springer, Berlin.

Dennis, H., Bergmo, P. & Holt, T. 2005: Tilted oil–water contacts: modelling the effects of aquifer heterogeneity. In: Doré, A.G. & Vining, B.A. (eds), Petroleum geology: North-West Europe and global perspectives. Proceedings of the 6th Petroleum Geology Conference, 145–158. The Geological Society, London. https://doi.org/10.1144/0060145

Esbensen, K.H. & Geladi, P. 2010: Principles of proper validation: use and abuse of re-sampling for validation. Journal of Chemometrics 24, 168–187. https://doi.org/10.1002/cem.1310

Esbensen, K.H. & Swarbrick, B. 2018: Multivariate data analysis. 6th edition, 462 pp. Camo software, Oslo.

Galluccio, L., Foote, N., Bertouche, M., Kostic, B. & James, A. 2019: Preliminary assessment of dolomite stringers in the Upper Jurassic Farsund Formation as a potential unconventional hydrocarbon reservoir. In: Patruno, S., Archer, S.G., Chiarella, D., Howell, J A., Jackson, C.A.-L. & Kombrink, H. (eds), Cross-Border Themes in Petroleum Geology I: The North Sea. Geological Society, London, Special Publication 494, 12 pp. https://doi.org/10.1144/SP494-2018-184

Goffey, G., Attree, M., Curtis, P., Goodfellow, F., Lynch, J., Mackertich, D., Orife, T. & Tyrrell, W. 2018: New exploration discoveries in a mature basin: offshore Denmark. Geological Society, London, Petroleum Geology Conference series 8, 287–306. https://doi.org/10.1144/pgc8.1

Gradstein, F.M., Ogg, J.G., & Hilgen, F.J. 2012: On the geologic time scale. Newsletters on Stratigraphy 45, 171–188. https://doi.org/10.1127/0078-0421/2012/0020

Gradstein, F.M., Ogg, J.G., Schmitz, M. & Ogg, G. (eds) 2014: The geologic time scale. eBook ISBN: 9780444594488, Paperback ISBN: 9780444594259. Elsevier.

Hemmet, M. 2005: The hydrocarbon potential of the Danish Continental Shelf. In: Doré, A.G. & Vining, B.A. (eds), Petroleum geology: North-West Europe and global perspectives, 85–97. Proceedings of the 6th Petroleum Geology Conference. Geological Society, London. https://doi.org/10.1144/0060085

Ineson, J.R. & Surlyk, F. (eds) 2003, The Jurassic of Denmark and Greenland. Geological Survey of Denmark and Greenland Bulletin 1, 948 pp. https://doi.org/10.34194/geusb.v1

Ineson, J.R., Bojesen-Koefoed, J.A., Dybkjær, K. & Nielsen, L.H. 2003: Volgian–Ryazanian 'hot argillaceous shales' of the Bo Member (Farsund Formation) in the Danish Central Graben, North Sea: Stratigraphy, facies and geochemistry. Geological Survey of Denmark and Greenland Bulletin 1, 403–436. https://doi.org/10.34194/geusb.v1.4679

Japsen, P. 1998: Regional velocity-depth anomalies, North Sea chalk: A record of overpressure and Neogene uplift and erosion. AAPG Bulletin 82, 2031–2074. https://doi.org/10.1306/00aa7bda-1730-11d7-8645000102c1865d

Japsen, P., Britze, P. & Andersen, C. 2003: Upper Jurassic–Lower Cretaceous of the Danish Central Graben: Structural framework and nomenclature. Geological Survey of Denmark and Greenland Bulletin 1, 1–49. https://doi.org/10.34194/geusb.v1.4653

Johannessen, P.N., Dybkjær, K., Andersen, C., Kristensen, L., Hovikoski, J. & Vosgerau, H. 2010: Upper Jurassic reservoir sandstones in the Danish Central Graben: New insights on distribution and depositional environments. Petroleum Geology Conference series 7, 127–143. https://doi.org/10.1144/0070127

Justwan, H., Dahl, B., Isaksen, G.H. & Meisingset, I. 2005: Late to Middle Jurassic source facies and quality variations, South Viking Graben, North Sea. Journal of Petroleum Geology 28, 241–268. https://doi.org/10.1111/j.1747-5457.2005.tb00082.x

Kubala, M., Bastow, M., Thomsen, S., Scotchman, I. & Oygard, K. 2003: Geothermal regime, petroleum generation and migration. In: Evans, D., Graham, C., Armour, A. & Bathurst, P. (editors and compilers), The Millennium Atlas: Petroleum Geology of the Central and Northern North Sea. 289–315. Geological Society of London, Bath, London.

Lokhorst, A. (ed.) 1997: NW European Gas Atlas. NITG-TNO (Haarlem). 154 pp. Available from: https://www.nlog.nl/sites/default/files/nw%20european%20gas%20atlas.pdf

Magoon, L.B. & Dow, W.G. (eds) 1994: The petroleum system — from source to trap. AAPG Memoirs 60, 645 pp. Tulsa, Oklahoma.

Michelsen, O., Nielsen, L.H., Johannessen, P.N., Andsbjerg, J. & Surlyk, F. 2003: Jurassic lithostratigraphy and stratigraphic development onshore and offshore Denmark. Geological Survey of Denmark and Greenland Bulletin 1, 147–216. https://doi.org/10.34194/geusb.v1.4651

Minkkinen, P. 1987: Evaluation of the fundamental sampling error in the sampling of particulate solids. Analytica Chimica Acta 196, 237–245. https://doi.org/10.1016/s0003-2670(00)83089-5

Møller, J.J. & Rasmussen, E.S. 2003: Middle Jurassic – Early Cretaceous rifting of the Danish Central Graben. Geological Survey of Denmark and Greenland Bulletin 1, 247–264. https://doi.org/10.34194/geusb.v1.4654

Müller, S., Arfai, J., Jähne-Klingberg, F., Bense, F. & Weniger, P. 2020: Source rocks of the German Central Graben. Marine and Petroleum Geology 113, 104120, 15 pp. https://doi.org/10.1016/j.marpetgeo.2019.104120

Nielsen, S.B., Clausen, O.R. & McGregor, E. 2015: basin%Ro: A vitrinite reflectance model derived from basin and laboratory data. Basin Research 29, 515–536. https://doi.org/10.1111/bre.12160

Østfeldt, P. 1987: Oil source rock correlation in the Danish North Sea. In: Brooks, J. & Glennie, K. (eds), Petroleum Geology of North-West Europe, 419–429. Graham & Trotman, London.

Passey, Q.R., Creaney, S., Kulla, J.B., Moretti, F.J. & Stroud, J.D. 1990: A practical model for organic richness from porosity and resistivity logs. AAPG Bulletin 74, 1777–1794. https://doi.org/10.1306/0c9b25c9-1710-11d7-8645000102c1865d

Pedersen, S., Weibel, R., Johannessen, P. & Schovsbo, N.H. 2018: The diagenetic impact on reservoir sandstones of the Heno Formation in the Ravn-3 well, Danish Central Graben, Denmark. Geological Survey of Denmark and Greenland Bulletin 41, 9–12. https://doi.org/10.34194/geusb.v41.4330

Pepper, A.S. & Corvi, P.J. 1995: Simple kinetic models of petroleum formation: Part III. Modelling an open system. Marine and Petroleum Geology 12, 417–452. https://doi.org/10.1016/0264-8172(95)96904-5

Peters, K.E. 1986: Guidelines for evaluating petroleum source rock using programmed pyrolysis. AAPG Bulletin 70, 318–329. https://doi.org/10.1306/94885688-1704-11d7-8645000102c1865d

Petersen, H.I. & Brekke, T. 2001: Source rock analysis and petroleum geochemistry of the Trym discovery, Norwegian North Sea: A Middle Jurassic coal-sourced petroleum system. Marine and Petroleum Geology 18, 889–908. https://doi.org/10.1016/s0264-8172(01)00033-2

Petersen, H.I. & Hertle, M. 2018: A review of the coaly source rocks and generated petroleums in the Danish North Sea: An underexplored Middle Jurassic petroleum system? Journal of Petroleum Geology 41, 135–154. https://doi.org/10.1111/jpg.12697

Petersen, H.I. & Nytoft, H.P. 2007a: Are Carboniferous coals from the Danish North Sea oil-prone? Geological Survey of Denmark and Greenland Bulletin 13, 13–16. https://doi.org/10.34194/geusb.v13.4964

Petersen, H.I. & Nytoft, H.P. 2007b: Assessment of the petroleum generation potential of Lower Carboniferous coals, North Sea: Evidence for inherently gas-prone source rocks. Petroleum Geoscience 13, 271–285. https://doi.org/10.1144/1354-079306-723

Petersen, H.I. & Rosenberg, P. 1998: Reflectance retardation (suppression) and source rock properties related to hydrogen-enriched vitrinite in Middle Jurassic coals, Danish North Sea. Journal of Petroleum Geology 21, 247–263. https://doi.org/10.1306/bf9ab7a6-0eb6-11d7-8643000102c1865d

Petersen, H.I., Rosenberg, P. & Andsbjerg, J. 1996: Organic geochemistry in relation to the depositional environments of Middle Jurassic coal seams, Danish Central Graben, and implications for hydrocarbon generative potential. AAPG Bulletin 80, 47–62. https://doi.org/10.1306/64ed873c-1724-11d7-8645000102c1865d

Petersen, H.I., Andsbjerg, J., Bojesen-Koefoed, J.A., Nytoft, H.P. & Rosenberg, P. 1998: Petroleum potential and depositional environments of Middle Jurassic coals and non-marine deposits, Danish Central Graben, with special reference to the Søgne Basin. Geological Survey of Denmark Bulletin 36, 81 pp. https://doi.org/10.34194/dgub.v36.5022

Petersen, H.I., Andsbjerg, J., Bojesen-Koefoed, J.A. & Nytoft, H.P. 2000: Coal-generated oil: source rock evaluation and petroleum geochemistry of the Lulita oilfield, Danish North Sea. Journal of Petroleum Geology 23, 55–90. https://doi.org/10.1111/j.1747-5457.2000.tb00484.x

Petersen, H.I., Nielsen, L.H., Bojesen-Koefoed, J.A., Mathiesen, A., Kristensen, L. & Dalhoff, F. 2008: Evaluation of the quality, thermal maturity and distribution of potential source rocks in the Danish part of the Norwegian–Danish Basin. Geological Survey of Denmark and Greenland Bulletin 16, 66 pp. https://doi.org/10.34194/geusb.v16.4989

Petersen, H.I., Nytoft, H.P., Vosgerau, H., Andersen, C., Bojesen-Koefoed, J.A. & Mathiesen, A. 2010: Source rock quality and maturity and oil types in the NW Danish Central Graben: Implications for petroleum prospectivity evaluation in an Upper Jurassic sandstone play area. Petroleum Geology Conference series 7, 95–111. https://doi.org/10.1144/0070095

Petersen, H.I., Holme, A.C., Thomsen, E., Whitaker, M.F., Brekke, T., Bojesen-Koefoed, J.A., Hansen, K.H. & Larsen, B.T. 2011: Hydrocarbon potential of Middle Jurassic coaly and lacustrine and Upper Jurassic–lowermost Cretaceous marine source rocks in the Søgne Basin, North Sea. Journal of Petroleum Geology 34, 277–304. https://doi.org/10.1111/j.1747-5457.2011.00506.x

Petersen, H.I., Andersen, C., Holme, A.C., Carr, A.D. & Thomsen, E. 2012: Vitrinite reflectance gradients of deep wells with thick chalk sections and high pressure: Implications for source rock maturation, Danish-Norwegian Central Graben, North Sea. International Journal of Coal Geology 100, 65–81. https://doi.org/10.1016/j.coal.2012.06.006

Petersen, H.I., Holme, A.C., Andersen, C., Whitaker, M.F., Nytoft, H.P. & Thomsen, E. 2013: The source rock potential of the Upper Jurassic – lowermost Cretaceous in the Danish southern Norwegian sectors of the Central Graben, North Sea. First Break 31, 43–53. https://doi.org/10.3997/1365-2397.2013011

Petersen, H.I., Hertle, M., Juhasz, A. & Krabbe, H. 2016: Oil family typing, biodegradation and source rock affinity of liquid petroleum in the Danish North Sea. Journal of Petroleum Geology 39, 247–268. https://doi.org/10.1111/jpg.12645

Petersen, H.I., Hertle, M. & Sulsbrück, H. 2017: Upper Jurassic-lowermost Cretaceous marine shale source rocks (Farsund Formation), North Sea: Kerogen composition and quality and the adverse effect of oil-based mud contamination on organic geochemical analyses. International Journal of Coal Geology 173, 26–39. https://doi.org/10.1016/j.coal.2017.02.006

Petersen, H.I., Hillock, P., Milner, S., Pendlebury, M. & Scarlett, D. 2019: Monitoring gas distribution and origin in the Culzean field, UK Central North Sea, using data from a continuous isotope logging tool and isotube and test samples. Journal of Petroleum Geology 42, 435–450. https://doi.org/10.1111/jpg.12745

Ponsaing, L., Bojesen-Koefoed, J.A., Thomsen, E. & Stemmerik, L. 2018: Temporal organic facies variations of Upper Jurassic – lowermost Cretaceous source rocks in the Danish Central Graben, North Sea. International Journal of Coal Geology 195, 217–237. https://doi.org/10.1016/j.coal.2018.06.006

Ponsaing, L., Petersen, H.I., Bojesen-Koefoed, J.A., Nytoft, H.P., Schovsbo, N.H. & Stemmerik, L. 2020a: Source rock quality variations of Upper Jurassic – lowermost Cretaceous marine shales and their relationships to oils in the Valdemar Field, Danish North Sea. Journal of Petroleum Geology 43, 49–74. https://doi.org/10.1111/jpg.12749

Ponsaing, L., Mathiesen, A., Petersen, H.I., Bojesen-Koefoed, J.A., Schovsbo, N.H., Nytoft, H.P. & Stemmerik, L. 2020b: Organofacies composition of Upper Jurassic – lowermost Cretaceous source rocks, Danish Central Graben, and insight into the correlation to oils in the Valdemar Field. Marine and Petroleum Geology 114, 104239, 22 pp. https://doi.org/10.1016/j.marpetgeo.2020.104239

Rasmussen, E.S., Piasecki, S., Andsbjerg, J., Dybkjær, K., Vejbæk, O.V., Jacobsen, C., Britze, P. & Bryde-Auken, M. 2005: Cenozoic maps of the Danish North Sea area. GEUS Report 2005/33, 8 pp, 19 figures.

Schenk, O., Peters, K.E. & Burnham, A.K. 2017: Evaluation of

Alternatives to Easy%Ro for Calibration of Basin and Petroleum System Models. 79th EAGE Conference and Exhibition volume 2017. 1–5. https://doi.org/10.3997/2214-4609.201700614

Schovsbo, N.H., Thomsen, E., Nytoft, P. & Esbensen, K. 2018: Oil maturity, families and oil-source rock correlations in the Danish North Sea based on biomarker studies. 80th EAGE Conference & Exhibition volume 2018, 1–5 pp. https://doi.org/10.3997/2214-4609.201801491

Schovsbo, N.H., Ladage, S., Mathiesen, A., Nelskamp, S. Stewart, M.A. & Britze, P. 2020: Unconventional hydrocarbon resource plays in the North Sea Basin, Northwestern Europe. EGU General Assembly 2020. EGU2020-1558, 1 p. https://doi.org/10.5194/egusphere-egu2020-1558

Smithson, T. 2016: HPHT wells. The defining series. Oilfield Review 2016, Schlumberger, 2pp.

Sweeney, R.E. & Burnham, A.K. 1990: Evaluation of a simple model of vitrinite reflectance based on chemical kinetics. AAPG Bulletin 74, 1559–1570. https://doi.org/10.1306/0c9b251f-1710-11d7-8645000102c1865d

Taylor, G.H., Teichmüller, M., Davis, A., Diessel, C.F.K., Littke, R. & Robert, P. 1998: Organic Petrology, 704 pp. Bornträger, Berlin, Stuttgart.

Thomsen, E., Damtoft, K. & Andersen, C. 1987: Hydrocarbon plays in Denmark outside the Central Trough. In: Brooks, J. & Glennie, K.W. (eds), Petroleum Geology of North-West Europe, 375–388. Graham & Trotman, London.

Thomsen, E., Lindgreen, H. & Wrang, P. 1983: Investigation on the source rock potential of Denmark. In: Kaasschieter J.P.H. & Reijers T.J.A. (eds), Petroleum Geology of the southeastern North Sea and the adjacent onshore areas, 221–239. Springer, Dordrecht. https://doi.org/10.1007/978-94-009-5532-5_21

Thomsen, R.O., Lerche, I. & Korstgård, J.A. 1990: Dynamic hydrocarbon predictions for the northern part of the Danish Central Graben: An integrated basin analysis assessment. Marine and Petroleum Geology 7, 123–137. https://doi.org/10.1016/0264-8172(90)90036-g

van Buchem, F.S.P., Smit, F.W.H., Buijs, G.J.A., Trudgill, B. & Larsen, P.-H. 2017: Tectonostratigraphic framework and depositional history of the Cretaceous–Danian succession of the Danish Central Graben (North Sea) – new light on a mature area. Geological Society, London, Petroleum Geology Conference series 8, 9–46. https://doi.org/10.1144/pgc8.24

Vejbæk, O.V. 2008: Disequilibrium compaction as the cause for Cretaceous–Paleogene overpressures in the Danish North Sea. AAPG Bulletin 92, 165–180. https://doi.org/10.1306/10170706148

Vejbæk, O.V., Bidstrup, T., Britze, P., Erlström, M., Rasmussen, E.S. & Sivhed, U. 2007: Chalk depth structure maps, Central to Eastern North Sea, Denmark. Geological Survey of Denmark and Greenland Bulletin 13, 9–12. https://doi.org/10.34194/geusb.v13.4962

Vejbæk, O., Frykman, P., Bech, N. & Nielsen, C.M. 2005: The history of hydrocarbon filling of Danish chalk fields. In: Doré, A.G. & Vining, B.A. (eds), Petroleum geology: North-West Europe and global perspectives, 1331–1345. Proceedings of the 6th Petroleum Geology Conference. London: Geological Society. https://doi.org/10.1144/0061331

Verreussel, R.M.C.H., Bouroullec, R., Munsterman, D.K., Dybkjær, K., Geel, C.R., Houben, A.J.P., Johannessen, P.N. & Kerstholt-Boegehold, S.J. 2018: Stepwise basin evolution of the Middle Jurassic–Early Cretaceous rift phase in the Central Graben area of Denmark, Germany and The Netherlands. Geological Society, London, Special Publication 469, 305–340. https://doi.org/10.1144/sp469.23

Waples, D.W., Pedersen, M.R. & Kuijpers, P. 2004: Correction of Single Log-Derived Temperatures in the Danish Central Graben, North Sea. Natural Resources Research 3, 229–239. https://doi.org/10.1007/s11053-004-0131-8